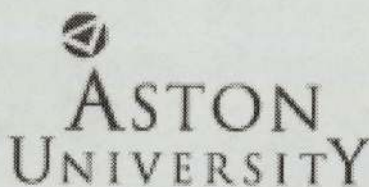


**Investigation of a binding model
for anti-cancer cyclohexadienones
by computational chemistry and crystallography**

Ruobo Ren

Master of Philosophy



July 2005

This copy of the thesis has been supplied on condition that anyone who consults it is understood to recognise that its copyright rests with its author and that no quotation from the thesis and no information derived from it may be published without proper acknowledgement.

Summary

A series of aryl-substituted quinols have shown good anti-cancer activity, and the crystal structure of the benzothiazole-substituted compound had recently been determined in the Aston University laboratory. The geometry of the reactive cyclohexadienone ring in this structure and related molecules in the Cambridge Structural Database has been surveyed.

The allowable steric relationship between this ring and the benzothiazole ring has been investigated by molecular modelling.

Thioredoxin is believed to be the biological target, with two of its cysteine thiol groups attacking the double bonds of the quinol ring. The geometry and stability of model adducts in which thiols bind to the cyclohexadienone ring in the possible alternative orientations have been compared.

The geometry and thermodynamics of thioredoxin binding have been modeled.

The previously determined crystal structure of a related quinol in which the aryl substituent is an indole derivative had been seriously affected by twinning. A higher-quality specimen crystal has been found and used to collect twice the required unique set of data, enabling reliable comparison of the two independent molecules in the asymmetric unit to be made.

As a path-finding project an improved specimen crystal was found and used for the amidrazone DLR944. This structure also has two independent molecules in the asymmetric unit, and a previous data set had given unrealistic displacement parameters for a t-butyl group. The new data set gives a more credible picture.

To my Parents and sister

Acknowledgements

I would like to express my sincere thanks to my supervisor Dr. Carl H. Schwalbe, who provided me with priceless guidance, advice and encouragement for the completion of this project.

I also point out my appreciation to Dr. Dan L. Rathbone, who offered me the demonstration of the relevant software technology and any help needed on the research project.

Finally, I am grateful for the assistance of the computer officer Mr. John Williams and other staff in the School of Life and Health Sciences in the Aston University.

contents

Summary	2
Dedication	3
Acknowledgement	4
Contents	5
Tables	8
Figures	9
Abbreviations	11
1 Introduction	13
<u>1.1 Molecular modelling</u>	13
1.1.1 Background	13
1.1.2 Molecular orbital methods	14
1.1.2.1 <i>Ab initio</i> molecular orbital methods	15
1.1.2.2 Approximate molecular orbital theories	16
1.1.2.3 Semi-empirical methods	16
1.1.3 Molecular mechanics	19
1.1.3.1 A simple molecular mechanics force field	20
1.1.3.2 Some general features of molecular mechanics force fields	21
1.1.4 Molecular modelling Application	24
<u>1.2 Anti-cancer quinols</u>	24
<u>1.3 X-ray crystallography</u>	28
2 Experiments	30
Part I Molecular modelling studies on AW464 using CAChe3.2	30
<u>2.1 Introduction</u>	30
2.1.1 Preparing a chemical sample file	31
2.1.2 Choosing a property class	31

2.1.3	Choosing a property	31
2.1.4	Choosing a procedure	33
<u>2.2</u>	<u>Material and Apparatus</u>	33
2.2.1	Material	33
2.2.2	Apparatus	33
<u>2.3</u>	<u>Data collection</u>	34
Part II Crystallography of Multi-ring Compounds Including		
	an Anti-cancer Quinol	34
<u>2.4</u>	<u>Introduction</u>	34
<u>2.5</u>	<u>Materials and instruments</u>	36
2.5.1	Materials	36
2.5.2	Instruments	36
<u>2.6</u>	<u>Data collection</u>	37
2.6.1	General	37
2.6.2	Structure redetermination and refinement	37
3	Results and Discussion	38
Part I Molecular Modelling studies on AW464 using CAChe 3.2		
<u>3.1</u>	<u>Survey of cyclohexadienone ring geometry in available crystal structures</u>	38
<u>3.2</u>	<u>The steric relationship between the cyclohexadienone ring and the benzothiazole ring of AW464</u>	39
<u>3.3</u>	<u>“Double Michael” adducts with simple thiols</u>	40
3.3.1	Nucleophilic susceptibility values	48
<u>3.4</u>	<u>Modelling of thioredoxin adducts</u>	53
Part II	Crystallography of anti-cancer quinols	58

3.5	<u>Crystal structure redeterminations</u>	58
3.5.1	The anti-cancer quinol JMB033	58
3.5.2	Crystal structure refinement of DLR944	65
3.6	<u>Comparison between AW464 X-Crystallography and AW464 with</u> <u>MA/MP</u>	67
4.	Conclusion	73
	References	75
	Appendices	82
Appendix I.	Results of a Cambridge Structural Database search for cyclohexadienone derivatives	83
Appendix II.	Crystallographic results for compound BW114 from crystal sample JMB033	84
Appendix III.	Crystallographic results for compound DLR944 from crystal sample DR944RFR	102

Tables

Table 1.	Adducts with one or two thiomethyl groups	42
Table 2.	Adducts of simple dithiols by MM3/AM1	44
Table 3.	Nucleophilic Susceptibility of AW464 and its adducts.	48
Table 4.	A variety of adducts of AW464 with the relevant Cys-Gly-Pro-Cys fragment	54
Table 5.	Selected bond distances (with estimated standard deviations on the line below) for the two independent molecules of JMB033 compared with those in AW464.	59
Table 6.	Torsion angles in the linkages between rings	60
Table 7.	X-ray crystallographic distances showing a significant difference	63
Table 8.	X-ray crystallographic bond angles showing a possibly significant difference	63
Table 9.	Hydrogen bond geometry	63
Table 10.	Selected torsion angles	64
Table 11.	Selected experimental and calculated bond distances	68
Table 12.	Selected experimental and calculated bond angles	69
Table 13.	Selected experimental and calculated torsion angles	70

Figures

Figure 1.	Structure of AW464, 2a, 22-hydroxytingenone (NSC 684506), heliangolide (NSC 335753) and arnebin (NSC 140377)	26
Figure 2	Bragg equation diagram	29
Figure 3.	Structure of JMB033	35
Figure 4.	Structure of DLR944	36
Figure 5.	O vs. C deviation from plane	39
Figure 6.	Structure of AW464 with atom numbering	39
Figure 7	Diagram to explain the nomenclature U1, D1, U2, D2, UU and DD	40
Figure 8.	Ball and Cylinder models of SCH ₃ D 1 MM3/AM1 and SCH ₃ D 1 MM3/PM3	43
Figure 9.	Ball and Cylinder models of S- (CH ₂) ₂ -S DD MM3/AM1 and S- (CH ₂) ₂ -S DD MM3/PM3 and S- (CH ₂) ₂ -S UU MM3/AM1 and S- (CH ₂) ₂ -S UU MM3/PM3	47
Figure 10.	Structure of AW464 with atom numbering by CaChe	48
Figure 11.	Ball and Cylinder models of DD C15 U MA and DD C15 U MP	50
Figure 12.	Nucleophilic susceptibility comparison graph of No. 1 to 20 models in table 4 on C12 of Figure 7	52
Figure 13.	Nucleophilic susceptibility comparison graph of No. 1 to 20 models in table 4 on C14 of Figure 7	52
Figure 14.	Ball and Cylinder model of DD/Cys35 -C15 D-Cys32-C11D	56
Figure 15.	Space Filling model of Thioredoxin adduct with hybrid	

PM3/MM optimization	57
Figure 16. Crystallography structure of JMB033 and AW464	63
Figure 17. Crystallography structure of old DLR944 and refined DLR944.	66

Abbreviations

AM1	(Austin Model 1) Dewar's NDDO semiempirical parameterization.
AMBER	Assisted Model Building and Energy Refinement
CNDO	(Complete Neglect of Differential Overlap) The simplest of the semi-empirical methods. The principal feature is the total neglect of overlap between different orbitals. In other words, the overlap matrix <i>S</i> is the unit matrix. The only two-electron integrals kept are those where electron 1 is in just one orbital and electron 2 is in just one orbital. Like all semi-empirical methods the integrals are evaluated empirically.
Cys	Cysteine
Gly	Glycine
INDO	Intermediate neglect of differential overlap
MM	(Molecular Mechanics) classical description of molecules as atoms held together by spring-like bonds. Chemical "Hamiltonian" based on force constants.
MM2	(Molecular Mechanics, Allinger Force Field version 2) one of the earliest, and probably the best known and tested Molecular Mechanics force field for organic molecules.
MM3	(Molecular Mechanics, Allinger Force Field version 3)
MINDO/3	(Modified Intermediate Neglect of Differential Overlap version 3) Refers to the parametrization set (and computer code) developed by the Dewar group for performing INDO calculations. The most useful of the MINDO series is MINDO/3.
MNDO	(Modified Neglect of Diatomic Overlap) Dewar's first parametrization of the NDDO semi-empirical method. First incorporated into the MOPAC program.
NCI	National Cancer Institute
NDDO	(Neglect of Differential Diatomic Overlap) This semi-empirical method that keeps all terms of the Fock matrix except those involving diatomic differential overlap: the only two-electron

terms, are those where $e^- 1$ is in one orbital on atom A and $e^- 2$ is in one orbital on atom B.

PM3 (Parametric Method number 3) A re-parameterized version of AM1 by Stewart.

Pro Proline

UV Ultraviolet

1. Introduction

1.1 Molecular Modelling

1.1.1 Background

What is molecular modelling? The Oxford English Dictionary defines 'model' as 'a simplified or idealised description of a system or process, often in mathematical terms, devised to facilitate calculations and predictions'. Molecular modelling would seem to be relevant to ideas of imitating the actions of molecules and molecular systems. Modern molecular modelling indicates computer modelling, even though profitable primitive work was done through utilizing solid models and calculation by hand. Computational sciences have led revolutions in molecular modelling to the extent that only a computer can perform most calculations. Such highly-developed models are sometimes worse than advanced elementary ones, however computers have of course expanded the scope of models considered and systems to be applied.^{1,2}

It is time to be a systematization that computational sciences can apply to pharmaceutical research. Recent improvements in computing have aided a variety of techniques, both new and old, to mature into missiles against disease. Molecular informatics: theoretical chemistry or molecular modelling, bio-informatics, after chemo-informatics, is now of true benefit within drug invention. Computer-assisted molecular design has contributed to the design and development of potent *in vitro* lead molecules as well as clinically useful agents (i. e., drugs).^{2, 3-12}

But 40% of human disease remains incurable and a lot of existing therapies are far from ideal. Not less than in the West, the character of disease has drastically diversified during the last century and is likely to be continuing. This plays a difficult and on-going confrontation both with the pharmaceutical industry and with the science available to undertake it. An unprecedented information explosion will be delivered by the post-genomic revolution-genomics, transcriptomics, and proteomics-compounded by High Throughput Screening, and the coming revolution of lab-on-chip super-synthesis. We will be able to manage and fully exploit this data overload only by informatics strategies.²

1.1.2 Molecular orbital methods

Generally, *ab initio* methods show molecular orbitals as linear combinations of atomic orbitals (LCAO). The basis set of atomic orbitals normally is composed of all shells up to and including the valence shell and may be even more universal. Both all practical *ab initio* methods and all more approximate methods rely on the Born-Oppenheimer approximation: because the heavy nuclei move much more slowly than the light electrons, for calculations involving electrons the nuclei are assumed to be stationary. The electrons are assumed to generate a time-averaged potential if properties of the nuclei are calculated.²

1.1.2.1 *Ab initio* Molecular Orbital Methods

Performing and understanding for closed-shell systems, which have no partly filled shells or unpaired electrons, by *ab initio* calculations is more uncomplicated. The Roothaan-Hall equations, which for a closed-shell system are: $FC=SC\epsilon$ in matrix notation, provide an approach that can be efficiently coded into computer programs. Matrix elements refer to the atomic orbitals in the basis set. The Fock matrix F is derived from the Hamiltonian operator, which in principle determines the wave function and the energy. However, the Hamiltonian operator includes electron-electron repulsion. This repulsion can only be calculated once the wave function is known, yet it is needed to calculate the wave function. The Fock approach overcomes this difficulty by using an average repulsion term. The other variables in the Roothaan-Hall equations are straightforward: C is a matrix of coefficients, S is the overlap matrix and ϵ is the energy matrix.

In order to build the matrices, large numbers of integrals must be calculated. These difficult computations result from the mathematical nature of the wave functions for the atomic orbitals used in the basis set. On the other hand, to integrate Gaussian functions (which produce the bell-shaped curves familiar in statistics) is easier. Therefore a short series of Gaussian functions, typically from 3 to 6 is used to express each atomic orbital in the widely used *ab initio* programs such as GAMESS and GAUSSIAN. *Ab initio* methods have become a widely used computational tool through the improvements in computer hardware and the availability of such easy to use programs.

1.1.2.2 Approximate Molecular Orbital Theories

But, in terms of the computer resources required, *ab initio* calculations can be extremely expensive. Significantly less computational resources are used by the approximate quantum mechanical methods. Undoubtedly, certain carefully chosen properties can be calculated more accurately by the earliest approximate methods than the highest level of *ab initio* methods.

A series of approximate molecular orbital theories have been formulated. The more widely used methods of today are derived from them although most of the early methods are no longer much applied. It is well known that the semi-empirical methods were developed in the research groups of Pople and Dewar. Pople's group originated the CNDO, INDO and NDDO methods, which are now rarely applied in their primary style but supplied the foundation for subsequent work by the Dewar group, whose research resulted in the conventional MINDO/3, MNDO and AM1 methods. An alternative development by Stewart led to the PM3 method. One aim of this thesis will be to evaluate how the AM1 and PM3 implementations of the theory can be applied in a practical way, not only to highlight their successes but also to show where problems were encountered.¹

1.1.2.3 Semi-empirical methods

The key components of the Roothaan-Hall equations, which for a closed-shell system are FC=SCE, are considered as a comparison of semi-empirical with *ab initio* methods firstly. It was clear that the number of arithmetical operations

required to investigate even the simplest of systems would be very large when the ideas of *ab initio* molecular orbital calculations were first developed. Therefore, to neglect or approximate some of these integrals is the most obvious way to decrease the computational effort since most of these operations have the purpose of calculating and manipulating integrals. Explicitly considering only the valence electrons of the system has partly achieved this using semi-empirical method; electrons occupying inner shells are considered together with the nuclear core. The theory behind this approximation is that the electrons involved in chemical bonding are those in the valence shell. An improvement on earlier theories such as Huckel theory that explicitly consider only the π electrons of a conjugated system and which are therefore limited to specific classes of molecule is through considering all the valence electrons of the semi-empirical methods. Atomic orbitals simplified to Slater type s, p and sometimes d orbitals are the basic sets used in semi-empirical calculations. These orbitals are orthogonal, allowing further simplifications to be made to the equations.¹³

S represents the overlap matrix in the Roothaan-Hall equations. Integrating the product of their wave functions over all space calculates the matrix element corresponding to any two atomic orbitals. This overlap matrix, S, is set equal to the identity matrix I in a feature common to the semi-empirical methods. Therefore all diagonal elements of the overlap matrix, corresponding to the product of a wave function with itself, are equal to 1 and all off-diagonal elements are zero. Some of the off-diagonal elements would naturally be zero because of the use of orthogonal basis sets on each atom. But, the matrix elements corresponding to the overlap between two atomic orbitals on different atoms are also set to zero. The Roothaan-

Hall equations simplified: $FC=SCE$ becomes $FC=CE$ as the main implication of this and so is immediately in standard matrix form. At first sight this assumption appears very foolish because the entire explanation of covalent bonding arises from the overlap of orbitals on different atoms. It is important to mark that overlap is still considered in calculating the elements of the Fock matrix F . Setting S equal to the identity matrix does not mean that corresponding overlap integrals are set to zero in the calculation of Fock matrix elements. In fact, including some of the overlaps in even the simplest of the semi-empirical models is important specifically.¹

Calculating other interactions of orbitals through empirical parameters chosen to make the results fit experimental or higher-quality theoretical results achieve further simplification. This is the explanation calling it a semi-empirical approach. Parameters are required for every element in a system, except for bond lengths, bond angles, etc. CNDO was the first semi-empirical approach, where *ab initio* calculations developed to the required parameters. The results were rather good, and could be calculated rapidly if the great simplifications were used. Dewar tried a similar approach called MINDO/3. Dewar followed the alternative principle of parameterising the method from experimental data instead of from *ab initio* calculations. This program was further advanced and called MNDO, and then AM1. An alternative development is PM3. These semi-empirical methods are available both in a package called MOPAC and in a number of other commercial and academic programs.¹³⁻²⁰

It was possible to calculate the necessary integrals for more than the very smallest of molecules when more powerful computers appeared. People gave up the semi-

empirical approach and went back to slower but more accurate *ab initio* methods. Dewar continued the semi-empirical approach, and these programs are very broadly applied to a wide variety of researches. Dewar's final publication on the subject indicated that a hybrid semi-empirical *ab initio* approach might be best.²⁰⁻²²

The speed resulting from the simplifications to the integrals is the chief advantage of semi-empirical molecular orbital programs over *ab initio* molecular orbital programs. Also a subsidiary advantage occurs. Because methods such as AM1 and PM3 are parameterized in agreement with experimental results, and the experimental results contain the effects of electron correlation, some allowance for this effect is implicit in the calculations. This can also be considered as a disadvantage, because it is not obvious now how great an allowance is being made for this effect, and so it is very puzzling to assess the errors in the method.¹³

1.1.3 Molecular Mechanics

To quantum mechanics, many problems to be studied in molecular modelling are unfortunately too large to be considered. Quantum mechanical methods deal with the electrons in a system, so that a large number of particles must still be considered even if some of the electrons are omitted (as in the semi-empirical schemes), and the calculations are time-consuming. Molecular mechanics, also known as force field methods, provided faster results. By discarding all the quantum mechanical ideas of electrons in orbitals, these procedures treat a molecule by classical mechanics as a system of balls (atoms) and springs (bonds). Parameters are now required for bond lengths, bond angles, etc. Being so firmly tied to experimental

data, results are often very good for molecules similar to those from which the parameters were derived but at risk of significant error for other types of molecules. Calculations are so quick that they are feasible for macromolecules. It can safely be said that molecular structure, and the accuracy in calculating molecular properties frequently matches the results that can be got experimentally. But, because it does not consider electrons and orbitals, molecular mechanics is unable to supply properties that depend on the electronic distribution in a molecule.^{1, 23-34}

The validity of several assumptions make that molecular mechanics works at all. The Born-Oppenheimer approximation, already discussed, which makes it possible to write the energy as a function of the nuclear coordinates, is the first of these. Processes such as the stretching of bonds, the opening and closing of angles and the rotations about single bonds are assumed to contribute to the global energy. The force field can perform quite acceptably even when simple functions like Hooke's law for bond stretching are used to describe these contributions. Transferability is highly admirable in a force field, since it allows parameters developed and tested on a few simple model molecules to be applied to a much wider range of problems and to much larger molecules such as polymers.¹

1.1.3.1 A simple molecular mechanics force field

It became possible to apply force fields to problems of interest to chemists when computers became commercially available in the 1950s. In the 1960s, early molecular mechanics programs were developed. A lot of the molecular modelling force fields in use today can be interpreted in terms of just four components of the intra- and inter- molecular forces within the system. Energetic drawbacks are

associated with the deviation of (1) bonds and (2) angles away from their 'reference' or 'equilibrium' values, there is a function that describes how the energy changes (3) as bonds are rotated, and finally the force field contains terms that describe (4) the interaction between non-bonded parts of the system. More sophisticated force fields may have additional terms, but they always include these four components. A useful feature of this representation is that the energy conversions due to changes in specific internal coordinates such as bond lengths, angles, and the rotation of bonds or movements of atoms relative to each other can be evaluated. It is easier to understand by this how changes in the force field parameters affect its performance and thus helps in the parameterization process. Once the parameters have been set, the main factors causing a particular conformation of a molecule to have a high energy can be identified. If this conformation is necessary for a drug to bind to a receptor, the harmful features can be designed away.^{1, 35-39}

1.1.3.2 Some general features of molecular mechanics force fields

Both the functional form and also the parameters define a force field. Two force fields may have the same functional form yet use very different parameters. It is totally possible that force fields with the same functional form but different parameters, and force fields with different functional forms, may give results of comparable accuracy. It is essential that a force field should be regarded as a single entity. It is not strictly correct to separate the energy into its individual components, and it is unsafe to take some of the parameters from one force field and mix them with parameters from another force field. However, some of the terms in a force

field are sufficiently independent of the others (particularly the bond and angle terms) to allow them to be considered on their own in certain cases.¹

The force fields used in molecular modelling are usually designed to replicate structural properties. Because UV-visible spectra depend on transitions of electrons between orbitals, molecular mechanics force fields can seldom predict spectra reliably (although the more recent molecular mechanics force fields are much better in this aspect). A force field is mainly designed to predict certain properties and will be parameterized accordingly. While it is a bonus if it predicts other quantities that have not been included in the parameterization process, a force field should not be discarded if it is unable to do so.¹

Transferability of the functional form and parameters is highly admirable in a force field. With transferability the same set of parameters can be used to model a series of linked molecules, rather than having to define a new set of parameters of each individual molecule. For example, the same set of parameters should be valid for all n-alkanes. Transferable force fields can be applied to make predictions. Only for some small systems, where particularly accurate work is required, may be admirable to develop a model specific to that molecule.¹

Force fields are empirical, and so there is no 'correct' form. The selection of a force field is based on performance. The fact that most of the force fields in common use do have a very similar form indicates that this may therefore be the best functional form. Such models do provide a useful image of the interactions present in a system, but it is always possible that there may be better forms, particularly when

developing a force field for new classes of molecule. The functional forms employed in molecular mechanics force fields are often a compromise between accuracy and computational productivity. Fulfilling the highest accuracy may be incompatible with efficient computation. When the performance of computers increases so it becomes possible to make the models more sophisticated. Molecular mechanics calculations are frequently used to seek minimum energy conformations. The search for minima by techniques like energy minimization and molecular dynamics usually requires calculation of the first and second derivatives of the energy with respect to the atomic coordinates. Easy calculation of derivatives then becomes an significant feature.

Most force fields use the concept of an atom group. The input for a quantum mechanics calculation demands the atomic numbers and positions of the nuclei present, together with the overall charge and spin multiplicity. For a force field the global charge and spin multiplicity are not explicitly required, but it is usually necessary to assign an atom type to each atom in the system. The atom group usually encodes more information than just the atomic number of an atom. Its hybridization state and sometimes the local environment are defined as well. For instance, it is necessary in most force fields to distinguish between tetrahedral sp^3 -hybridised carbon atoms, trigonal sp^2 -hybridised carbons and linear sp -hybridized carbons. Each force field parameter is expressed in terms of these atom groups. Therefore the reference angle θ° for a tetrahedral carbon atom would be near 109.5° and that for a trigonal carbon would be near 120° . The atom groups in some force fields reflect the local environment as well as the hybridization and can be quite extensive for some atoms. For example, the MM2, MM3 and MM4 force fields of

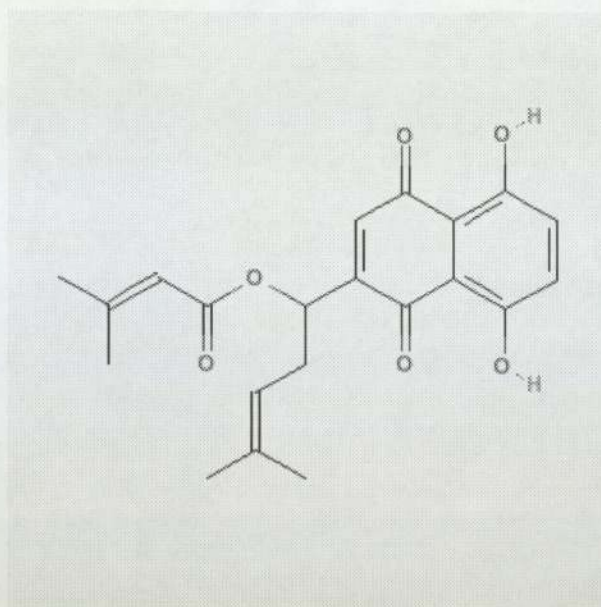
Allinger and co-workers that are widely used for calculations on 'small' molecules distinguish the following groups of carbon atom: sp^3 , sp^2 , sp , carbonyl, cyclopropane, radical, cyclopropene and carbonium ion. In the AMBER force field of Kollman and co-workers the carbon atom at the junction between a six- and a five-membered ring (e.g. in the amino acid tryptophan) is assigned an atom group that is different from the carbon atom in an isolated five-membered ring such as histidine, which in turn is different from the atom type of a carbon atom in a benzene ring. Other, more general, force fields would assign these atoms to the same generic ' sp^2 carbon' atom group. Force fields which are designed for modelling specific classes of molecule (such as proteins and nucleic acids, in the case of AMBER) often use more specific atom types than force fields designed for general-purpose use.^{1, 40-51}

1.1.4 Molecular modelling Application

The present study starts from the crystal structure of AW464 determined in our laboratory.⁵² and relies on the conclusion from database mining of the NCI 60 cell screening panel suggesting that the protein thioredoxin is its target. Human thioredoxin (1ERT in the Protein Data Bank) has two active-site cysteine residues at positions 32 and 35 with S atoms only 3.9 Å apart.⁵³ Their proximity suggests that they could attack the cyclohexadienone ring of the drug in a 'double Michael addition.'

1.2 Anti-cancer quinols

4-Hydroxy-4-(benzothiazol-2-yl)cyclohexadienone (AW464) is a highly active member of a set of aryl-substituted quinols that show selectivity against renal and colon cancer cell lines.⁵⁴



arnebin (NSC 140377)

Figure 1. Structure of AW464, 2a, 22-hydroxytingenone (NSC 684506), heliangolide (NSC 335753) and arnebin (NSC 140377)

When the aromatic portion of such a molecule is a fused heterobicyclic structure (e.g., benzothiazole derivative AW464 (NSI 706704)), potent *in vitro* antitumor activity was observed in HCT 116 (GI₅₀=40 nM) and HT 29 (GI₅₀= 380 nM) human colon as well as in MCF-7 and MDA 468 human breast cancer cell lines.⁵⁴

When examined on the NCI Developmental Therapeutics Screening Program *in vitro* screen (60 human cancer cell lines), active compounds in this series consistently displayed a highly unusual pattern of selectivity; cytotoxicity (LC₅₀) was concentrated in certain colon and renal cell lines only.⁵⁴ AW464 also showed *in vivo* antitumor activity against human RXF 944XL renal xenografts in nude NMRI mice and is the focus of further study.⁵⁴

An early lead compound was the acetoxy derivative called 2a (NSC 696142) which showed potent activity in the National Cancer Institute (NCI) in vitro 60-cell panel (mean GI₅₀=0.36 μ M).⁵⁴ It was shown that 2a is unstable in cell culture media, undergoing rapid hydrolysis to AW464, a compound with a similar antitumor profile to 2a.⁵⁴ LC-MS was used to determine that the major degradation product of 2a (mass 285) was AW464 (mass 243).⁵⁴ Considering the rapid breakdown of 2a to AW464 and the similar activity fingerprint indicates that the hydroxyl compound AW464 is the true bioactive species.⁴² Thus the former is acting as a prodrug modification of the latter.⁵⁴

The sharply defined pattern of anti-cancer selectivity for AW464 showed a degree of similarity to other compounds.⁵⁴ These included the natural products 22-hydroxytingenone (NSC 684506), heliangolide (NSC 335753), and arnebin (NSC 140377), together with many small synthetics characterized chemically as being "double Michael acceptors".⁵⁴ Of particular interest are structurally unrelated inhibitors of thioredoxin/thioredoxin reductase that possess similar profiles of in vitro antitumor activity, being toxic to colon, renal, and certain breast cancer cell lines.⁵⁵

"Michael addition is the nucleophilic addition of carbanions to α , β -unsaturated carbonyl compounds."⁵⁶

This definition can be stretched to include other nucleophiles such as the SH groups considered in the present study.

Most of the research reported here is based on molecular modelling: computer-based models were constructed for AW464 in alternative conformations, for Michael adducts with model thiols, and finally for adducts with thioredoxin. After initial coordinates were provided from the results of X-ray crystallography or by drawing the molecule, minimum-energy conformations were searched for. Initially the geometry was improved by using molecular mechanics. The search for minimum energy was continued with semi-empirical quantum mechanical calculations, by either AM1 or PM3. The relative success of these two alternatives will be evaluated.

1.3 X-ray crystallography

X-ray crystallography involves the determination of structure by analysis of the diffraction pattern produced when a crystal is irradiated with x-rays. A crystal is a regular, repeating array of atoms, molecules or ions. The crystals described in this thesis are composed of molecules. The repeat unit that generates the crystal is called the unit cell. Stacks of planes can be imagined to cut through the unit cell, intersecting an axis 0, 1, 2, or another integral number of times. While the mathematical analysis of three-dimensional diffraction is very complicated, it is equivalent to reflection off these planes. Reflection only occurs when $n\lambda=2d\sin\theta$, which is the condition for constructive interference between beams reflected from successive planes in the stack (**Figure 2**). Here n is an integer equivalent to the order of diffraction, usually 1, λ is the wavelength of the X-rays, d the perpendicular distance between planes, and θ the angle of incidence and reflection.

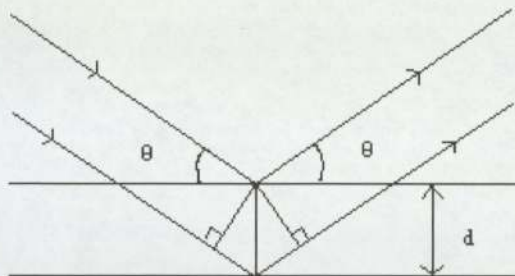


Figure 2. Bragg equation diagram

From measurement of θ values it is easy to work out the unit cell dimensions. From measurements of the intensity of reflection from each stack of planes it is possible to determine the structure and location of each molecule in the unit cell. However, the phase of each reflection must be supplied, and it cannot be measured. The phase of a wave determines whether a reference point is at a crest, a trough, or in between. Most frequently the phases are determined by a computerised process called direct methods. From these phases and the intensity data an electron density map can be calculated which shows where the atoms in the molecules are located. These positions are refined by least squares to give a final model that best fits the data.

High-quality results depend on having a truly regular crystal. If part of the molecule is vibrating strongly or has two or more alternative orientations (disorder), quality will be poor. If the crystal consists of two or more blocks usually related by rotation or reflection (twinning), the results will be strange. This thesis reports the successful redetermination of two structures for which the original data were unsatisfactory due to disorder and twinning.

2. Experiments

Part I Molecular Modelling studies on AW464 using CAChe 3.2

2.1 Introduction

CAChe can generate three-dimensional coordinates for a molecule from a drawing. To attach suitable numbers of hydrogen atoms to the carbon skeleton and to correct grossly distorted geometry, the “beautify” routine is available. After drawing and beautifying the original molecule in the workspace on the screen, it must be saved in a specified file name in a place chosen before doing any following property experiments. Although beautifying the molecule is expected to lower its energy to a reasonable value, there is no guarantee that this represents an energy minimum. Sequences of conformations are calculated from this chemical sample conformation and the best original saved structure file is found and copied to the new workspace. Then, the geometry optimisation property experiment is done by either MM/AM1 or MM/PM3 procedure. The nucleophilic susceptibility property is calculated with the same semi-empirical method that was used to optimize geometry, either at MM/AM1 geometry with AM1 wavefunction or MM/PM3 geometry with PM3 wavefunction procedure.

The following steps outline the process of performing a workspace experiment in this thesis.

2.1.1 Preparing a chemical sample file

Before performing an experiment, it is necessary to build and investigate the geometry of the molecule in a chemical sample file. Once all the constituent atoms and bonds of this molecule are drawn by the Atom/Bond tool in the workspace on the screen, the **Beautify/Comprehensive** menu option corrects valence, hybridization, geometry, and ring structure in one step. Chemical sample conformation experiments also require the addition of search labels through defining atom distances, bond angles, improper torsion angles, and dihedral angles depending on the objectives of a particular experiment.

2.1.2 Choosing a property class

Two classes of properties are used in the experiments and investigation:

chemical sample conformation properties

chemical sample properties

2.1.3 Choosing a property

Chemical sample conformation properties

Sequence of conformations

A sequence of conformations offers a fast method to arrive at purely low energy conformations by one pass search, which evaluates only one low energy value for each search label and is often an efficient way to get closer to the

global minimum energy value for a molecule. Sequential searches can only be performed by classical mechanical methods using an unlimited number of search labels in a sequence of conformation experiments.

Chemical sample properties

Optimized geometry

To discover low energy structures, the geometry of the chemical sample is optimized using semi-empirical quantum mechanics procedures AM1 or PM3. In optimizing a sample, the resulting low-energy geometry is based on the original starting geometry. It is better to perform a conformational search first and then optimize using the semi-empirical methods because these optimization procedures give local minima and it is only by chance that the global minimum would result from direct optimization of the input structure.

Susceptibility (nucleophilic)

The nucleophilic susceptibility is mainly influenced by the wave function for the lowest unoccupied molecular orbital (LUMO). Where its magnitude is large, an attacking nucleophilic reagent could easily insert surplus electrons into this empty orbital, and the nucleophilic susceptibility is high. CAChe creates a three-dimensional surface superimposed over the chemical sample at an electron density

of $0.01 \text{ e } \text{Å}^{-3}$ which indicates by colour the areas that are vulnerable to an attack by nucleophiles

2.1.4 Choosing a procedure

These procedures apply theories from classical mechanics or quantum mechanics to the chemical sample. The (most) accurate quantum mechanical procedure for a chemical sample is usually procedure MM/PM3 geometry with PM3 wavefunction, although depending on the sample, MM/AM1 geometry with AM1 wavefunction may sometimes yield better results. In both procedures a preliminary optimization by molecular mechanics provides a good starting point.

2.2 Material and Apparatus

2.2.1 Material

The present study starts from the crystal structure of AW464 determined in our laboratory.²

2.2.2 Apparatus

All of the modelling studies were carried out with the CAChe WorkSystem Version 3.2 in the CAChe Workspace (Copyright 1999 Oxford Molecular Ltd.). Intel

Pentium III processor 930 MHz, 256 MB of RAM computer with Microsoft Windows XP Professional system (Version 2002 Service Pack 2).

2.3 Data Collection

A geometry-optimized energy minimum for a chemical sample (heat of formation) is saved at mopac. log of the database in the folder called sample. io or shown temporarily at the list of calculations after the experiment. The geometry data are collected in the workspace by automatically showing when the atoms or bonds explored are highlighted and the bond geometries icons are chosen.

The Cambridge Structural Database was searched for cyclohexadienone derivatives in which the sp^3 tetrahedral bridgehead carbon atom is bonded to one C and one O atom, neither of which is part of a ring that could constrain the geometry.

Part II Crystallography of Multi-ring Compounds Including an Anti-cancer Quinol

2.4 Introduction

The Nottingham group has developed a second-generation anti-cancer cyclohexadienone drug.

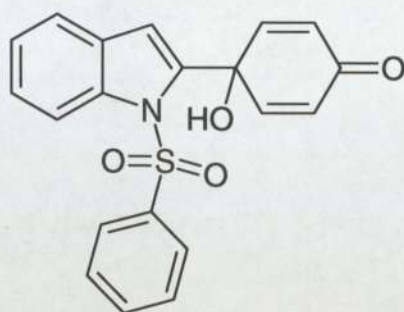


Figure 3. Structure of JMB033

From sample JMB033 the crystal structure was determined (C.H.Schwalbe, personal communication). The space group is $P2_1/c$ with unit cell dimensions $a=15.933(6)$, $b=13.449(2)$, $c=15.791(4)$ Å, $\beta = 99.22(2)^\circ$. However, this structure determination encountered two difficulties. Because the a and c axes have such similar lengths, the specimen crystal showed non-merohedral twinning relating $h k l$ and $l -k h$ reflections, which caused overlap of low-resolution reflections, separation at high resolution and partial overlap in between. For instance, the systematically absent $-8 0 3$ reflection was overlapped by the strong $-3 0 8$ from the twin component to give an apparent $F^2(\text{obs})=9039$. Refinement of a batch scale factor for the twin component in SHELXL-97 converged to 0.15. Furthermore, the presence of two molecules in the asymmetric unit instead of one placed greater demands on the refinement process. Therefore the present work was carried out to obtain more reliable data that would be less affected by twinning.

Because of the small quantity of crystals available, another crystalline compound (DLR944) with somewhat similar problems but a much bigger sample was initially

studied as a path-finding exercise. DLR944 is related to a series of compounds with activity against mycobacteria.

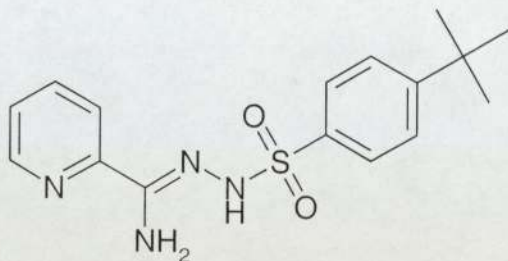


Figure 4. Structure of DLR944

It also has two independent molecules in the asymmetric unit. Although there is no problem with twinning this time, severe disorder in one of the terminal t-butyl groups resulted in difficult refinement (C. H. Schwalbe, personal communication) and unrealistic displacement parameters.

2.5 Materials and instruments

2.5.1 Materials

Samples of crystals were used as received from Prof. M. F. G. Stevens (JMB033) and Dr. D. L. Rathbone (DLR944).

2.5.2 Instruments

Crystals were carefully examined under a polarising microscope to find a specimen that had clearly defined faces and went sharply and uniformly dark when the

microscope stage was rotated. These features suggest a high-quality crystal with no twinning. All the crystal data were collected from an Enraf-Nonius CAD4 diffractometer with monochromated Mo-K α radiation, $\lambda=0.71069\text{\AA}$.

2.6 Data Collection

2.6.1 General

The ω - 2θ scan procedure was used for data collection between the limits $2^\circ \leq \theta \leq 25^\circ$. Three intensity and three orientation reflections were re-measured repeatedly to detect any decomposition (9% during 2 weeks of irradiation for both compounds) and slippage (negligible).

2.6.2 Structure redetermination and refinement

For JMB033 the previous trial structure was re-used. Full-matrix least-squares refinement varied the positions and anisotropic displacement parameters of all non-hydrogen atoms. Hydrogen atoms were assumed to ride on their attached atom with isotropic displacement parameters. Phase determination by direct methods gave a trial structure for DLR944 identical to the one determined previously. Procedures used for refinement were the same as those for JMB033.

3. Results and Discussion

Part I Molecular Modelling studies on AW464 using CAChe 3.2

3.1 Survey of cyclohexadienone ring geometry in available crystal structures.

Because 5 of its 6 carbon atoms take part in double bonds, the cyclohexadienone ring is expected to be fairly rigid and planar, but any flexibility in the cyclohexadienone ring and its substituents could facilitate its approach to a bulky macromolecular target. Instead of lying strictly in the plane defined by the two C=C bonds, the bridgehead carbon C8 of AW464 deviates by 0.06 Å from it.

To evaluate the extent of allowable deviations from this reference plane, the Cambridge Structural Database was searched for cyclohexadienone derivatives in which the sp³ tetrahedral bridgehead carbon atom is bonded to one C and one O atom, neither of which is part of a ring that could constrain the geometry. In the 12 structures found, the deviation of this carbon atom ranges from 0.01 to as much as 0.29 Å.

The deviations of the attached C and O atoms, when plotted against each other, lie almost on a straight line, suggesting that their motion rigidly follows that of the bridgehead carbon atom. In 11 of the 12 cases, as in AW464, the distortion brings the O atom nearer the plane. The data and REFCODE references are provided in the Appendix.

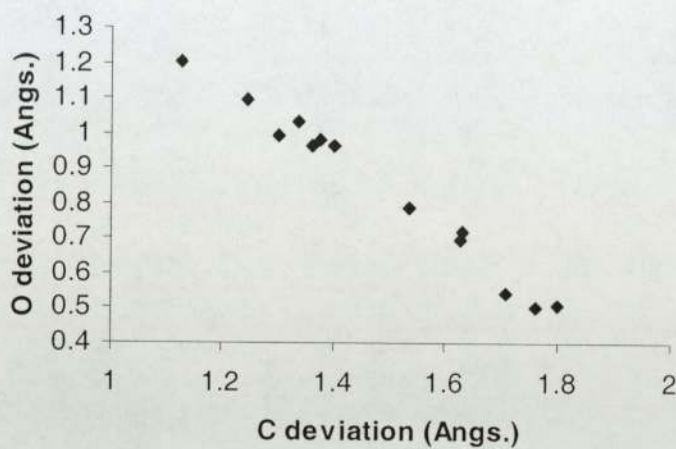


Figure 5. O vs. C deviation from plane

3.2 The steric relationship between the cyclohexadienone ring and the benzothiazole ring of AW464

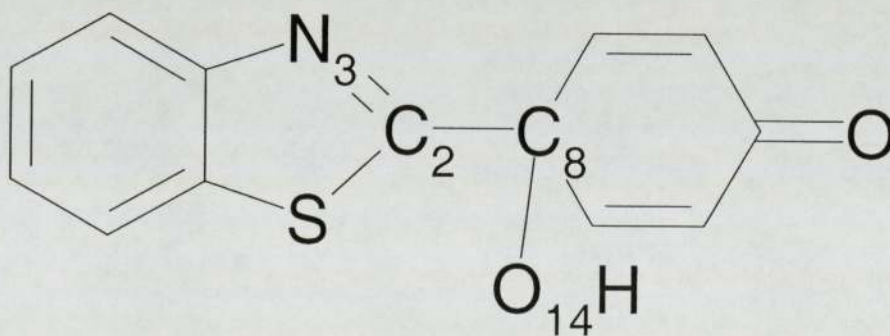


Figure 6. Structure of AW464 with atom numbering

In the crystal structure of AW464 the benzothiazole plane roughly bisects the cyclohexadienone ring: torsion angle N3-C2-C8-O14 is $-168.8(2)^\circ$, i.e. N3 is far

from O14. This torsion angle approaches 90° in a related indole derivative, suggesting free rotation, and therefore it was important to optimize it. At minimum energy after MOPAC MM3/PM3 optimization this torsion angle is -173.82° . The final heat of formation is 21.8kcal/mol. It should be noted that a conformation search before optimization, reported later, suggests that a different conformation would be more stable.

3.3 “Double Michael” adducts with simple thiols.

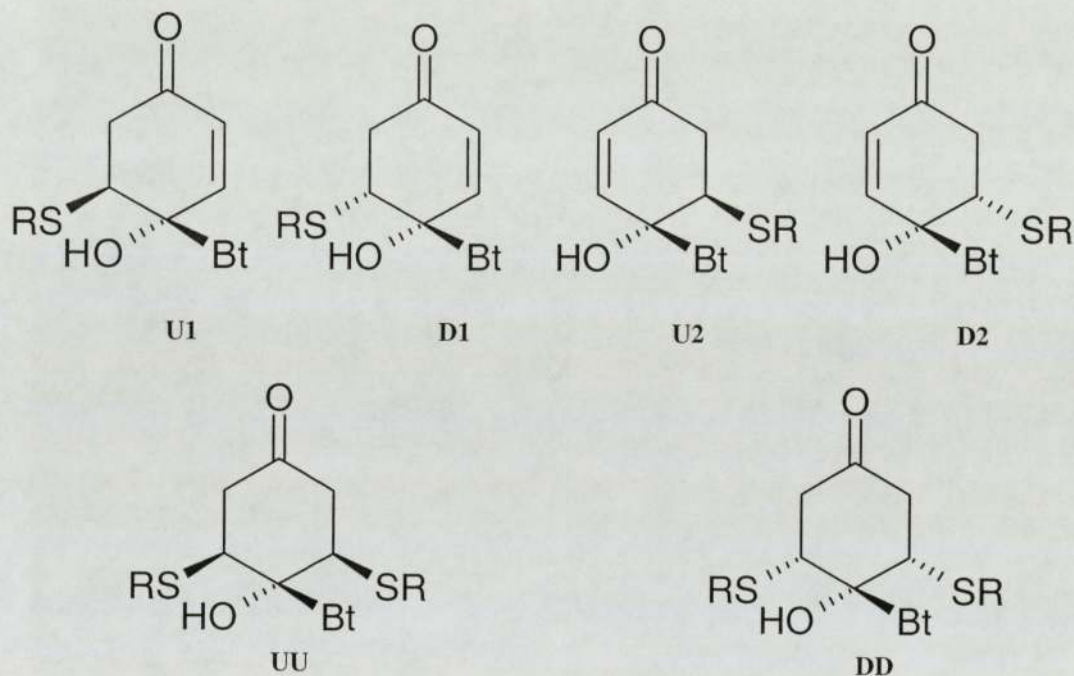


Figure 7. diagram to explain the nomenclature **U1**, **D1**, **U2**, **D2**, **UU** and **DD**

The U means the “up” which is defined by the original drawing stage in the workspace of the CaChe software as shown on **Figure 7**, either **U1** or **U2**. In other words, up means that the benzothiazole (Bt) ring is fixed and other binding adducts like SCH_3 , S-S, S- CH_2 -S, S- $(\text{CH}_2)_2$ -S or two SCH_3 approach the double bonds of the cyclohexadienone ring from that side of this ring, the top; and vice versa for down. The simplest model adduct has one SCH_3 group and one H atom added to

one double bond of the cyclohexadienone ring. Guided by the nucleophilic susceptibility calculations reported later, and in agreement with previous experience, the SCH₃ group is assumed to bind at the position beta to the carbonyl group, and the H atom at the alpha position. Alternative forms of attack by a single SCH₃ group occupy the first four rows in table 1. These models are built by combining the SCH₃ group with the appropriate atom on each of the two double bonds at the up and down position to that cyclohexadienone ring plane manually, and the double bond attacked by that SCH₃ group changes to a single bond before conformational searching is done. In fact the calculations with AM1 and PM3 agree that U attack by a single SCH₃ group yields a product lower in energy than the result of D attack. Labels 1 and 2 refer to the two double bonds which can be attacked. The energy differences (<=4 kcal/mol) between them are carried over from the asymmetry of the original crystal structure. SCH₃ D1 and SCH₃ D2 have the same energy value in the MM3/AM1 calculation due to their same absolute value of the N3-C2-C8-O14 torsion angle with opposite direction.

Further models were developed by adding an additional SCH₃ group and one H atom to the other double bond. The last four models have been built by combining the two SCH₃ groups with the atoms on both double bonds at the up and down position to the cyclohexadienone ring plane respectively and two double bonds change to two single bonds before doing conformational searching. Semi-empirical molecular orbital calculations with PM3 parameters unsurprisingly show Two SCH₃ DD diagram shown on **Figure 7**. to have a 6-kcal/mol lower heat of formation than Two SCH₃UU, although Two SCH₃UD achieves equal stability with ca. 90°

rotation of the benzothiazole ring. However, the AM1 results suggest that Two SCH₃UU is the most stable for reasons that are difficult to understand.

Table 1. Adducts with one or two thiomethyl groups

Name	MM3/AM1		MM3/PM3	
	N3-C2-C8-O14 torsion angle (degrees)	Energy value (Kcal/mol)	N3-C2-C8-O14 torsion angle (degrees)	Energy value (Kcal/mol)
SCH ₃ U1	-89.36	-12.78	-173.82	4.14
SCH ₃ U2	58.29	-8.75	-172.41	-0.64
SCH ₃ D1	55.86	-0.24	75.44	5.47
SCH ₃ D2	-55.86	-0.24	-80.47	7.01
Two SCH ₃	-177.18	-24.05	179.83	-13.27
DD				
Two SCH ₃	149.91	-19.26	141.19	-12.47
DU				
Two SCH ₃	75.97	-31.92	15.27	-12.43
UD				
Two SCH ₃	29.89	-36.59	83.80	-6.80
UU				

Figure 8 is one example of the models. In this case the two alternative optimization methods have yielded similar structures.



SCH₃ D 1 MM3/AM1

SCH₃ D 1 MM3/PM3

Figure 8. Ball and Cylinder models of SCH₃ D 1 MM3/AM1 and SCH₃ D 1 MM3/PM3

In these series of models the last four are apparently more stable than the first four. A true description of the reaction in balanced form is Quinol (Q) + thiol (T) = adduct QT. The energy change should be calculated by subtracting the energy of both reactants from the energy of the product. Since the energy of the isolated thiol is constant, comparisons between addition in alternative orientations can ignore it. The decrease in energy according to MM3/AM1 calculation is 7-36 kcal/mol and in MM3/PM3 calculation is 7-20 kcal/mol. This appears to be because the two SCH₃ groups release extra energy upon bond formation which outweighs the loss of conjugation in the system of double bonds in the cyclohexadienone ring. These two calculation parameters show here different model di-adducts to be the most stable. In MM3/AM1 the Two SCH₃UU is the most stable one, but in MM3/PM3 the Two SCH₃DD is the most stable one.

Adducts of simple dithiols were studied next to evaluate the importance of the extra constraint provided by linking the S atoms. A DD adduct (S-(CH₂)₂-S DD) of 1,2-

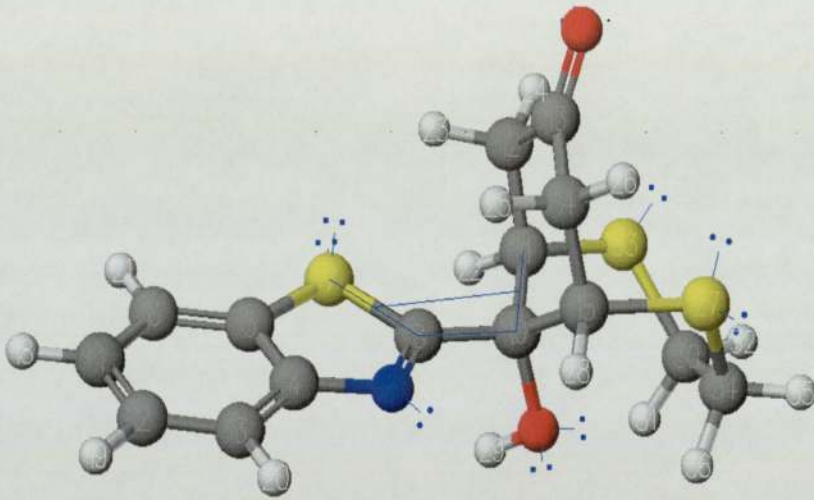
ethanedithiol with symmetrical C-S bonds and S...S contact of 3.30 Å can be built, although a less symmetrical structure with wider S...S contact is more stable.

Table 2. Adducts of simple dithiols by MM3/AM1 and MM3/PM3

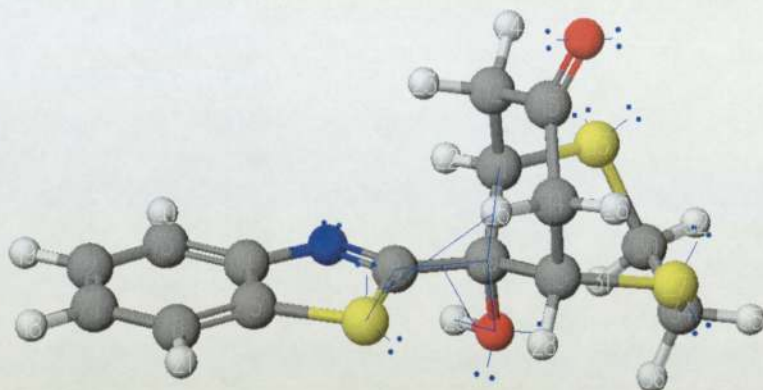
Procedure	Name	S-S UU	S-CH ₂ -S	S-(CH ₂) ₂ -S	S-(CH ₂) ₂ -S
			UU	DD	UU
MM3/AM1	S...S contact (Å)	2.19	2.96	3.15	3.64
	N ₃ -C2-C8-O14	-26.02	29.15	69.93	157.70
	torsion angle				
	(degrees)				
	Energy value	-8.75	-19.76	-8.89	-13.40
	(Kcal/mol)				
	Cyclohexanone	Chair	Chair	Chair (axial)	Twist boat
	ring geometry	(axial)	(axial)		
MM3/PM3	S...S contact (Å)	2.09	3.06	3.30	3.83
	N ₃ -C2-C8-O14	85.59	79.63	-74.25	99.69
	torsion angle				
	(degrees)				
	Energy value	12.40	3.34	8.35	2.63
	(Kcal/mol)				
	Cyclohexanone	Chair	Chair	Chair (axial)	Twist boat
	ring geometry	(axial)	(axial)		

In table 2, the molecules in the first two columns are built by combining the S-S or S-CH₂-S group with the atoms on two C=C double bonds at the up position to the

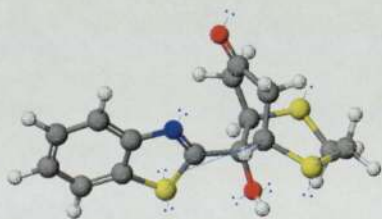
cyclohexadienone ring plane manually, and these two double bonds change to two single bonds before doing the conformational searching. The axially disubstituted chair conformation found for the cyclohexanone ring is normally not preferred, but here it permits the required close approach of the two S atoms. Even so, the S-S distance in the S-S adduct of 2.19 Å with AM1 and 2.09 Å with PM3 is longer than twice the 1.02 Å covalent radius tabulated from the Cambridge Structural Database (<http://www.ccdc.cam.ac.uk/products/csd/radii/>). The last two entries are built by the S-(CH₂)₂-S group combined with the same atoms as above at the up and down position to the same operation. At first sight the results seem surprising! AM1 and PM3 agree that UU is more stable than DD by about 5 kcal/mol. **Figure 9** compares two DD and two UU models. As is also implied by the analysis of ring geometry above, the DD adducts seem to have few problems with the cyclohexanone ring geometry. However, the S-(CH₂)₂-S group has an unfavourable eclipsed conformation. In the lower-energy UU models it appears that optimization has deformed the cyclohexanone ring sufficiently to allow the substituent to move to the opposite side of this ring from the benzothiazole. This deformation has also relieved the S-(CH₂)₂-S eclipse. The optimised UU structure has now seems to be DD. CAChe has been known to swap ring substituents if it leads to a lower energy, even though this is not physically possible.



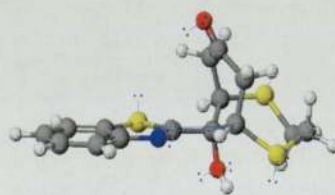
S- (CH₂)₂-S DD MM3/AM1



S- (CH₂)₂-S DD MM3/PM3



S- (CH₂)₂-S UU MM3/AM1



S- (CH₂)₂-S UU MM3/PM3

Figure 9. Ball and Cylinder models of S- (CH₂)₂-S DD MM3/AM1 and S- (CH₂)₂-S DD MM3/PM3 and S- (CH₂)₂-S UU MM3/AM1 and S- (CH₂)₂-S UU MM3/PM3

3.3.1 Nucleophilic susceptibility values

If the hypothesis is correct that thiol groups from thioredoxin carry out nucleophilic attack on the double bonds of AW464, the nucleophilic susceptibility should indicate which carbon atoms are likely to be attacked. The numbering scheme for the relevant carbon atoms is shown below.

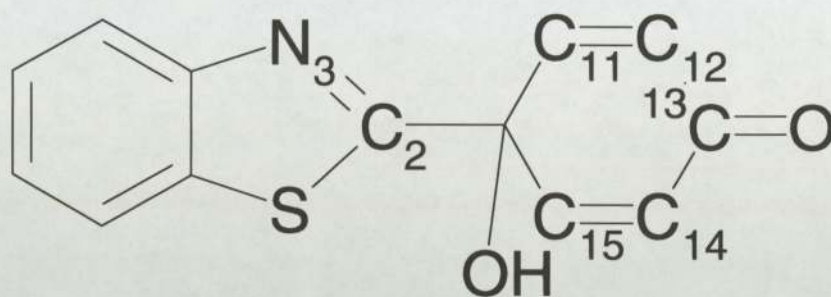


Figure 10. Structure of AW464 with atom numbering by CaChe

Table 3. Nucleophilic Susceptibility of AW464 and its adducts.

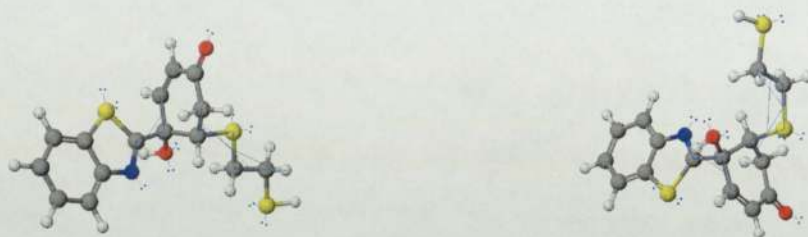
Name (procedure)	C11	C12	C13	C14	C15	N3-C2-C8-O14	Energy
	NS	NS	NS	NS	NS	torsion angle (degrees)	(Kcal/mol)
AW464. MA	0.2459	0.1410	0.2174	0.1048	0.2138	-71.50	21.72
AW464. MP	0.1607	0.0975	0.1373	0.0831	0.1483	99.69	21.76
SCH ₃ U1. MA	0.2253	0.1293	0.1391	0.0023	0.1095	-89.36	-12.78
SCH ₃ U1. MP	0.0871	0.0628	0.0390	0.0011	0.0289	-173.82	4.14
SCH ₃ D1. MA	0.1224	0.0852	0.0656	0.0002	0.0153	55.86	-0.24
SCH ₃ D1. MP	0.0568	0.0435	0.0279	0.0005	0.0105	75.44	5.47
SCH ₃ U2. MA	0.1961	0.1202	0.0790	0.0002	0.0097	58.29	-8.75
SCH ₃ U2. MP	0.0748	0.0477	0.0244	0.0003	0.0099	-172.41	-0.64
SCH ₃ D2. MA	0.0153	0.0002	0.0656	0.0851	0.1224	-55.80	-0.24
SCH ₃ D2. MP	0.0174	0.0003	0.0328	0.0481	0.0646	-80.47	7.01
TwoSCH ₃ DD. MA	0.0406	0.0017	0.0142	0.0018	0.0259	-177.18	-24.05
TwoSCH ₃ DD. MP	0.0594	0.0037	0.0094	0.0023	0.0320	179.83	-13.27
TwoSCH ₃ UU. MA	0.0833	0.0005	0.0166	0.0033	0.0886	29.89	-36.59
TwoSCH ₃ UU. MP	0.0256	0.0011	0.0029	0.0012	0.0173	83.80	-6.80

TwoSCH ₃	DU.	MA	0.0352	0.0015	0.0103	0.0007	0.0139	149.40	-19.26	
TwoSCH ₃	DU.	MP	0.0473	0.0024	0.0075	0.0023	0.0360	141.19	-12.47	
TwoSCH ₃	UD.	MA	0.1607	0.0016	0.0229	0.0011	0.0310	75.97	-31.92	
TwoSCH ₃	UD.	MP	0.0529	0.0035	0.0113	0.0032	0.1009	15.27	-12.43	
S-S UU.		MA	0.0156	0.0009	0.0058	0.0008	0.0228	-26.02	-8.75	
S-S UU.		MP	0.0377	0.0010	0.0007	0.0010	0.0332	85.59	12.40	
S-CH ₂ -S UU.		MA	0.1778	0.0008	0.0299	0.0016	0.0742	29.15	-19.76	
S-CH ₂ -S UU.		MP	0.0540	0.0015	0.0079	0.0019	0.0388	79.63	3.34	
1	S-(CH ₂) ₂ -S UU.	MA	0.0122	0.0013	0.0041		0.0121	157.70	-8.89	
2	S-(CH ₂) ₂ -S UU.	MP	0.0262	0.0008	0.0019	0.0014	0.0140	99.69	8.35	
3	S-(CH ₂) ₂ -S DD.	MA	0.0466	0.0006	0.0063	0.0005	0.0397	69.93	-13.40	
4	S-(CH ₂) ₂ -S DD.	MP	0.0572	0.0016	0.0068	0.0018	0.0422	-74.25	2.62	
5	DD.	C11D.	MA	0.1381	0.0037	0.1181	0.1065	0.1878	90.02	-11.99
6		C11D.	MP	0.0818	0.0021	0.0323	0.0450	0.0671	169.55	10.25
7		C11U.	MA	0.1381	0.0037	0.1180	0.1064	0.1877	90.30	-11.98
8		C11U.	MP	0.0656	0.0018	0.0327	0.0458	0.0679	165.10	9.13
9		C15D.	MA	0.1248	0.0870	0.0664	0.0003	0.0191	54.54	0.90
10		C15D.	MP	0.0583	0.0442	0.0288	0.0009	0.0217	76.79	11.26
11		C15U.	MA	0.1261	0.0873	0.0682	0.0004	0.0207	22.97	0.84
12		C15U.	MP	0.0579	0.0446	0.0279	0.0009	0.0224	73.89	11.75
13	UU.	C11D.	MA	0.0191	0.0003	0.0663	0.0867	0.1244	54.44	0.90
14		C11D.	MP	0.0222	0.0009	0.0280	0.0447	0.0581	73.56	11.26
15		C11U.	MA	0.1322	0.0037	0.1114	0.1015	0.1781	-90.08	-11.30
16		C11U.	MP	0.0432	0.0021	0.0383	0.0602	0.0835	-173.79	10.96
17		C15D.	MA	0.1265	0.0875	0.0683	0.0004	0.0206	-55.90	0.84
18		C15D.	MP	0.0658	0.0491	0.0333	0.0005	0.0283	-79.81	13.60
19		C15U.	MA	0.1781	0.1014	0.1116	0.0038	0.1330	90.04	-11.30
20		C15U.	MP	0.0664	0.0443	0.0321	0.0021	0.0823	168.02	10.25

MA=MM3/AM1 with AM1, MP=MM3/PM3 with PM3, NS= Nucleophilic susceptibility. If the adducts had mirror symmetry, the following pairs would be mirror images: 5,9; 6,10; 7,11; 8,12; 13,17; 14,18; 15,19; 16,20.

In table 3, the column DD and UU means that the models immediately following it are based on S-(CH₂)₂-S DD and S-(CH₂)₂-S UU respectively. Models C11D, C11U, C15D and C15U are built by breaking the bond linking the S-(CH₂)₂-S group to the named atom of the cyclohexanone ring and manually changing the S-(CH₂)₂-S group to the up or down position faced to the cyclohexanone ring before

conformational searching. The lack of mirror symmetry may be due to the original asymmetry of AW464 and the variability of manual intervention. This procedure provides an additional opportunity for molecules to reach low-energy conformations, as well as providing some insight into the intermediate that might be formed if the two thiol groups in thioredoxin bind in a stepwise manner.



DD C15 U MA

DD C15 U MP

Figure 11. Ball and Cylinder models of DD C15 U MA and DD C15 U MP

In the following discussion, the energy values in the right-hand column of Table 4 will first be compared with previous findings. Then the nucleophilic susceptibility as an index of reactivity will be examined.

In this database, the MM3/AM1 with AM1 calculation gives generally lower energy values, which may be thought to represent better data since the initial energy values for the unreacted AW464 were very similar.

As mentioned previously, comparison of energy values for AW464 and models of SCH_3 shows that the latter is more stable than the former, and models with two SCH_3 groups are lower still by an average of 10 kcal/mol. When the $\text{S}-(\text{CH}_2)_2\text{-S}$ adducts are detached at one end, the energy is expected to rise because of the loss

of the C-S and C-H bonds, although this effect may be offset by relief of strain. An energy increase is indeed observed for all the detached models based on DD. However, in model numbers 15 and 19 (designated in the leftmost column of Table 4) based on UU an energy decrease is found, suggesting that strain relief upon bond breaking may be important.

In unreacted AW464 there are high and fairly similar values of the nucleophilic susceptibility at C13, C11 and C15 (the carbonyl carbon atom and the two beta carbons in the double bonds). This supports the hypothesis of Michael addition. As double bonds become saturated, their nucleophilic susceptibility becomes small. In C11, C12 and C13 atoms, most nucleophilic susceptibility data in models of SCH₃ are higher than data in models of Two SCH₃ groups. This shows that the unreacted double bond in the cyclohexenone ring retains part of its original nucleophilic susceptibility. In turn this suggests that attack by a second nucleophile is possible, though apparently not as easy as the first attack.

This table also shows that nucleophilic susceptibility data of the S-(CH₂)₂-S DD models detached at one end (near the column DD in Table 4) are higher than data of the S-(CH₂)₂-S DD and S-(CH₂)₂-S UU. This is because one double bond has formed again in the cyclohexenone ring in those models.

There is a clear picture in which the nucleophilic susceptibility data at C15 atoms of C11D. MA, C11D. MP, C11U. MA, C11U. MP are higher than the data of C15D. MA, C15D. MP, C15U. MA, C15U. MP. This sign directs that the nucleophilic susceptibility will decrease after the C15 atom of the cyclohexenone ring is

attacked by the S- (CH₂)₂-S group in MA or MP modelling. There is the same situation in C12 and C14 data. So far the nucleophilic susceptibility seems to agree with the expected reactivity.

The data in C11 and C13 are not as pleasing as C12, C14 and C15 because the data about the former atoms are not regularly ordered, but C13 is not postulated to undergo addition anyway.

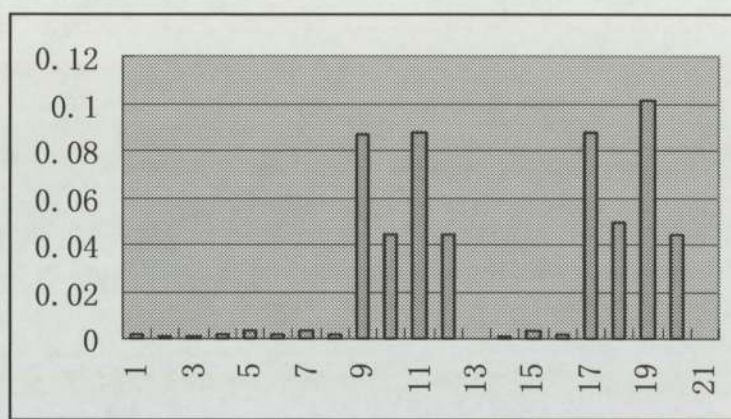


Figure 12. nucleophilic susceptibility comparison graph of No. 1 to 20 models in table 4 on C12 of Figure 7

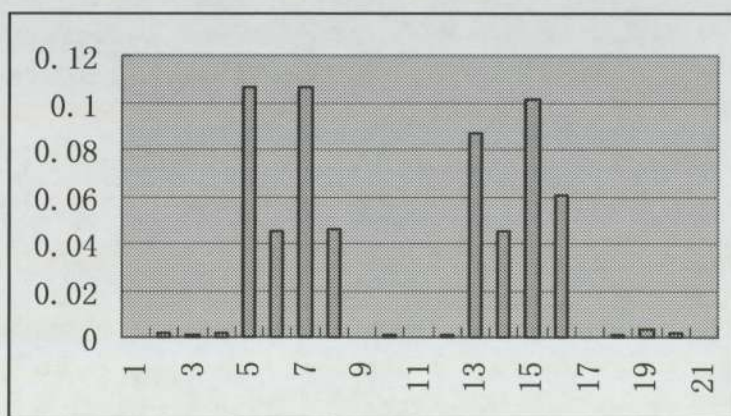


Figure 13. nucleophilic susceptibility comparison graph of No. 1 to 20 models in table 4 on C14 of Figure 7

Figure 11 and **Figure 13** show the nucleophilic susceptibility of AW464 S- (CH₂)₂-S adducts detached at one point, plotted against sequence numbers taken from the extreme left-hand column of the latter part of Table 4. The vertical axis shows the nucleophilic susceptibility. These two figures suggest when hydrogen atom capture is likely as a part of Michael addition. When the value at C12 is high, the value at C14 is low. The reverse is also true. Thus there is a clear directing effect for the addition of a hydrogen atom as well as the thiol.

3. 4 Modelling of thioredoxin adducts

There are 5 cysteine residues in thioredoxin. Of these, Cys32 and Cys35 are considered most likely to attack AW464 since they are placed at the active site with S...S distance only 3.9Å.²⁷ For an initial modelling study the Cys-Gly-Pro-Cys tetrapeptide from position 32 to position 35 of thioredoxin was used.

A model adduct of AW464 with the entire molecule of the complete thioredoxin molecule was subsequently constructed by Dr. D. L. Rathbone.

Optimisation with PM3 of the part of this model including AW464 and the relevant Cys-Gly-Pro-Cys fragment yields a structure with N3-C2-C8-O14 torsion angle - 122° and S...S contact 4.45 Å. In order to consider the full range of possibilities for binding of the tetrapeptide, i.e. “down” or “up” location for each Cys and connection at C11 or C15, optimizations were carried out as described in the table below.

	C15U					equatorial
UU.	Cys35 -	8.54	5.11	-96.42	-197.97	Cys35 axial,
	C15D-					Cys32
	Cys32-					equatorial
	C11D					
	Cys35-	8.18	4.93	-119.95	-192.21	Cys32 axial,
	C11D-					Cys35
	Cys32-					equatorial
	C15D					
	Cys35-	9.50	5.11	-93.72	-195.01	Cys35 axial,
	C15D-					Cys32
	Cys32-					equatorial
	C11U					
	Cys35-	8.82	4.61	-163.13	-193.28	Cys32
	C11D-					equatorial,
	Cys32-					Cys35 axial
	C15U					
	Cys35-	8.93	4.77	175.22	-195.79	Cys35
	C15U-					equatorial,
	Cys32-					Cys32 axial
	C11D					
	Cys35-	8.77	5.27	-100.84	-195.45	Cys32 axial,
	C11U-					Cys35
	Cys32-					equatorial
	C15D					
	Cys35-	5.76	5.39	-154.45	-192.58	● Twist-boat
	C15U-					
	Cys32-					
	C11U					
	Cys35-	6.79	4.58	179.60	-192.40	Cys32
	C11U-					equatorial,
	Cys32-					Cys35
	C15U					equatorial

D1=Distance between N in Benzothiazole ring and N Proline, D2=Distance 2

between N in Benzothiazole ring and O keto in Cyclohexanone ring

In table 4, the column DD and UU means that the following models nearby it are based on S-(CH₂)₂-S DD and S-(CH₂)₂-S UU before alteration as specified. The models following DD and UU are built by changing the S- (CH₂)₂-S group to the Cys-Gly-Pro-Cys fragment and are distinguished by the combined atoms at the two Cys groups (32 or 35) and the different atoms of the cyclohexanone ring (C11 or C15) to which they are connected. Ligands were attached at the up and down position to the cyclohexanone ring plane manually before doing conformational searching. This experiment is calculated by MM3/PM3 only.

Figure 14 is one example of models.

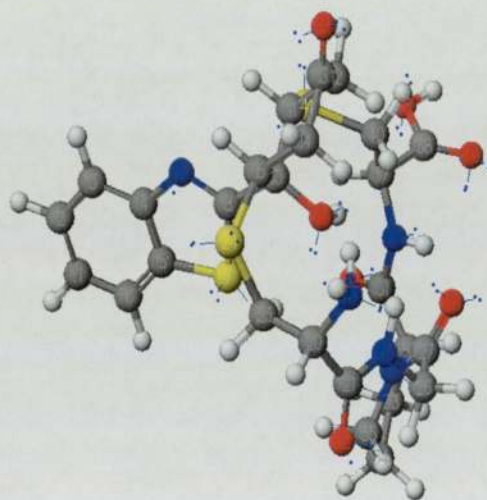


Figure 14. Ball and Cylinder model of DD/Cys35 -C15 D-Cys32-C11D

Conclusions from the geometrical features can be made about the presence or absence of bad contacts or distortion in the full thioredoxin adduct. The potential for such bad contacts is indicated in Table 5 by a black spot. If both the distance

between N in the benzothiazole ring and N in proline is 4-6 Å and the distance between N in the benzothiazole ring and O keto in the cyclohexanone ring is 5-6 Å, the contact of the two rings (benzothiazole ring and cyclohexanone ring) with the Cys-Gly-Pro-Cys fragment will lead to bad contact with further thioredoxin residues.

Figure 15 shows that the benzothiazole ring can insert into the pocket formed by the tetrapeptide, but this will not always happen when the tetrapeptide is linked to more peptides in thioredoxin. In the remaining models in table 5 with suitable N..N and N..O distances, the two rings are far away enough from the mouth formed by that tetrapeptide to avoid the bite.

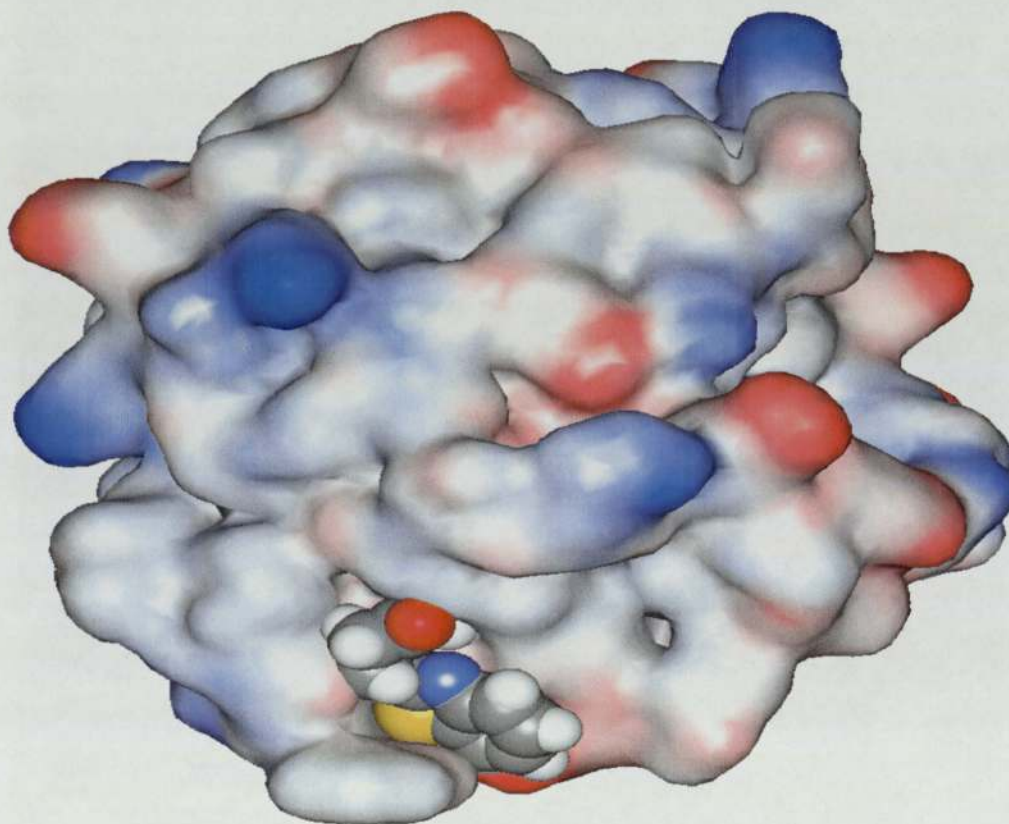


Figure 15. Space Filling model of Thioredoxin adduct with hybrid PM3/MM optimisation

This model is the result of further work by Dr. Dan L. Rathbone. A hybrid PM3/MM optimization of the full thioredoxin molecule, free drug and the thioredoxin adduct gives S...S contact of 4.41 Å in the adduct and positions the benzothiazole ring in a channel near an indole ring of tryptophan.

The calculated enthalpy change is +35 kcal/mol (only +11 kcal/mol with AM1 parameters), mainly due to distortion of the drug. However, the entropy increase from release of water may yet favor the reaction.

Part II Crystallography of anti-cancer quinols

3.5 Crystal structure redeterminations

3.5.1 The anti-cancer quinol JMB033

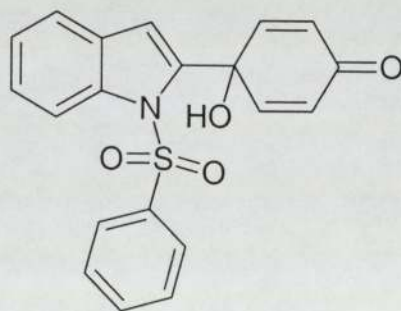


Figure 3. Structure of JMB033

The second-generation quinol JMB033 resembles the original AW464 in that both have a 6/5 heterocycle attached to the same quinol part. However, in JMB033 the heterocycle is an indole rather than a benzothiazole. Furthermore, this indole N atom bears an electron-withdrawing benzenesulfonyl substituent. Thus the heterocycle in JMB033 has considerably different steric requirements and some difference in electronic properties. Adding difficulty to the refinement is the existence of two independent molecules in the unit cell, labelled with primes in the left-hand molecule of JMB033 in **Figure 16** and unprimed in the right-hand molecule. However, it does provide an opportunity to compare the geometry.

Table 5. Selected bond distances (with estimated standard deviations on the line below) for the two independent molecules of JMB033 compared with those in AW464.

	JMB033		JMB033		AW464
	(left)		(right)		
C2'=C3'	1.342	C2=C3	1.345		
distances (Å)	(0.006)	distances (Å)	(0.006)		
C3a'=C7a'	1.390	C3a=C7a	1.389	C3a=C7a	1.397
distances (Å)	(0.006)	distances (Å)	(0.006)	distances (Å)	(0.003)
C4'=C5'	1.382	C4=C5	1.372	C4=C5	1.373
distances (Å)	(0.007)	distances (Å)	(0.008)	distances (Å)	(0.003)
C6'=C7'	1.384	C6=C7	1.384	C6=C7	1.374
distances (Å)	(0.007)	distances (Å)	(0.008)	distances (Å)	(0.003)
C9'=C10'	1.321	C9=C10	1.328	C9=C10	1.319
distances (Å)	(0.007)	distances (Å)	(0.006)	distances (Å)	(0.003)

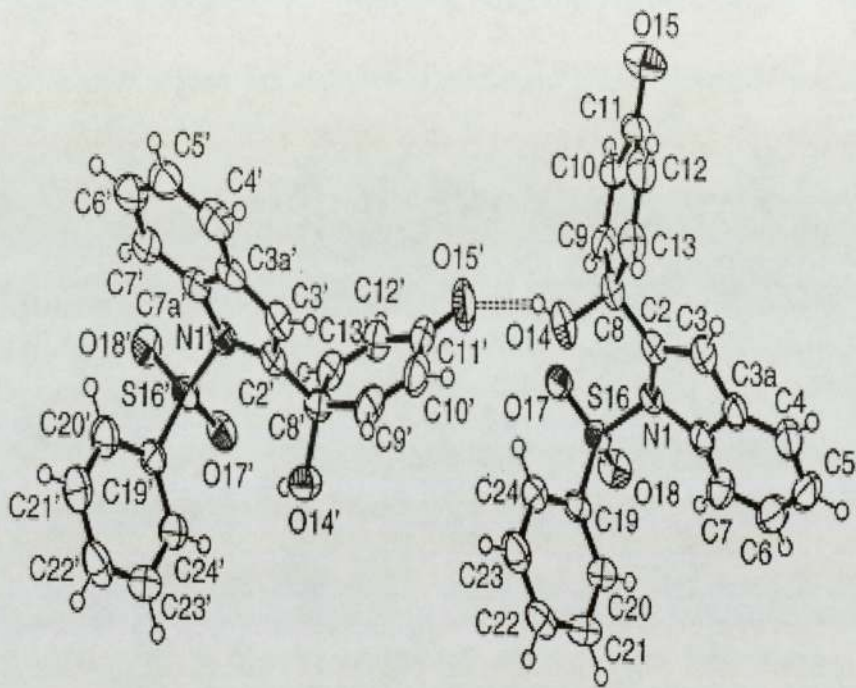
C12'=C13'	1.321	C12=C13	1.303	C12=C13	1.316
distances (Å)	(0.006)	distances (Å)	(0.006)	distances (Å)	(0.003)
C19'=C20'	1.381	C19=C20	1.389		
distances (Å)	(0.006)	distances (Å)	(0.006)		
C21'=C22'	1.375	C21=C22	1.384		
distances (Å)	(0.007)	distances (Å)	(0.007)		
C23'=C24'	1.378	C23=C24	1.385		
distances (Å)	(0.007)	distances (Å)	(0.006)		
C11'=O15'	1.234	C11=O15	1.230	C11=O15	1.224
distances (Å)	(0.006)	distances (Å)	(0.005)	distances (Å)	(0.003)

Table 6. Torsion angles in the linkages between rings

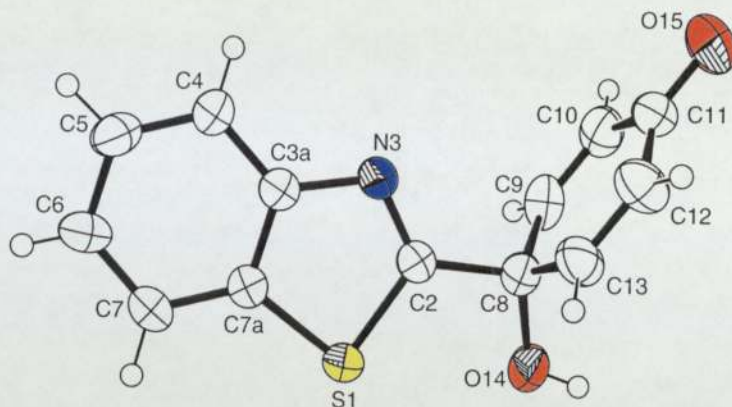
JMB033 (left)		JMB033 (right)	
N1'-C2'-C8'-O14'	-74.5 (0.5)	N1-C2-C8-O14	-68.3 (0.5)
Torsion angles (degrees)		Torsion angles (degrees)	
S16'-N1'-C2'-C8'	43.0 (0.5)	S16-N1-C2-C8	33.3 (0.5)
Torsion angles (degree)		Torsion angles (degrees)	
C7a'-N1'-C2'-C8'	-170.3 (0.4)	C7a-N1-C2-C8	-174.4 (0.3)
Torsion angles (degrees)		Torsion angles (degrees)	

In table 5 and 6, none of the C=C and C=O bond distances in the two independent molecules of JMB033 differ by as much as 3 standard deviations from each other or

from corresponding distances in AW464. Thus the cyclohexadienone rings should have similar reactivity. Torsion angles $\text{N1}'\text{-C2}'\text{-C8}'\text{-O14}'$, $-74.5 (0.5)^\circ$ and N1-C2-C8-O14 , $-68.3 (0.5)^\circ$ are quite similar with the AW464 torsion angle N3-C2-C8-O14 in table 4, -71.50° by MM3/AM1 and 99.69° by MM3/PM3. The latter value is related to the others by a rotation through approximately 180° . Also torsion angles involving the linkages between rings in JMB033 differ by $4\text{-}10^\circ$ between the two molecules. In effect, a single conformation is present in the crystalline state, subject to adjustment to accommodate the somewhat different crystal packing forces at the two sites. One obvious difference is the presence of a reasonably strong $\text{O14}'\text{-H}\dots\text{O17}'$ intramolecular hydrogen bond with $\text{H}\dots\text{O}$ contact 2.13 \AA in the left (primed) molecule, while the analogous contact in the right (unprimed) molecule is 2.67 \AA . However, both molecules form intermolecular $\text{O14}'\text{-H}\dots\text{O15}$ and $\text{O14-H}\dots\text{O15}'$ hydrogen bonds to the carbonyl O atom of the opposite molecule, the latter contact being shorter and straighter:



JMB033



AW464

Figure 16. Crystallography structure of JMB033 and AW464

Table 7. X-ray crystallographic distances showing a significant difference

Distance Å	X-Crystallography (JMB033 left)	Distance Å	X-Crystallography (JMB033 right)
C4'-C3a'	1.387 (0.006)	C4-C3a	1.409 (0.006)

Table 8. X-ray crystallographic bond angles showing a possibly significant difference

Angle (degrees)	(JMB033 left)	Angle (degrees)	(JMB033 right)
C2'-N1'-C7a'	106.5 (3)	C2-N1-C7a	107.2 (3)

Table 9. Hydrogen bond geometry

O14'-H14'	0.8200	O14-H14 Distance	0.8200
Distance (Å) (left)		(Å) (right)	

O14'-O15 Distance	2.927 (0.005)	O14-O15' Distance	2.759 (0.005)
(Å) (left)		(Å) (right)	
H14'-O15 Distance	2.345	H14-O15' Distance	1.996
(Å) (left)		(Å) (right)	
O14'-H14'-O15	128.5	O14-H14-O15'	154.5
Angle (degrees)		Angle (degrees)	
(left)		(right)	

Table 10. Selected torsion angles

Torsion angle	JMB033 (left)	Torsion angle	JMB033 (right)
(degrees)		(degrees)	
S16'-N1'-C2'-C8'	43.0 (0.5)	S16-N1-C2-C8	33.3 (0.5)
C3'-C2'-C8'-C13'	-116.6 (0.5)	C3-C2-C8-C13	5.6 (0.5)
N1'-C2'-C8'-C13'	50.7 (0.5)	N1-C2-C8-C13	177.9 (0.4)
C3'-C2'-C8'-C9'	5.0 (0.6)	C3-C2-C8-C9	-116.3 (0.4)
N1'-C2'-C8'-C9'	172.3 (0.4)	N1-C2-C8-C9	56.0 (0.5)
C2'-C8'-C13'-C12'	114.0 (0.5)	C2-C8-C13-C12	-119.6 (0.5)
O14'-C8'-C13'-C12'	-119.9 (0.5)	O14-C8-C13-C12	123.0 (0.5)
C2'-C8'-C9'-C10'	-115.9 (0.5)	C2-C8-C9-C10	116.6 (0.5)
O14'-C8'-C9'-C10'	124.23 (0.46)	O14-C8-C9-C10	-120.50 (0.45)

A batch scale factor for a twin component converged to 0.045 for this data set compared to 0.15 for the previous set. This slight amount of twinning may contribute to the differences in table 7 and 8, but the most likely cause is differences in conformation and packing. One is 10-245 degrees' difference of torsion angles data at groups of atoms in the cyclohexadienone ring of JMB033 left and JMB033 right and connected atoms in the indole ring, and the sulfur atom with N in the indole ring. The other is the variation in intermolecular distance shown in table 9.

In table 10, the torsion angles $N1'-C2'-C8'-C13'$, $50.7 (0.5)^\circ$, and $N1-C2-C8-C9$, $56.0 (5)^\circ$, are a lot more similar, so this can be explained by rearranging the cyclohexadienone ring numbering for one molecule.

3.5.2 Crystal structure refinement of DLR944

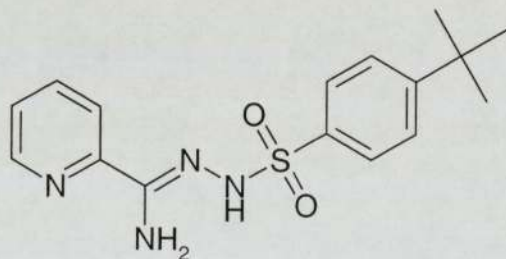
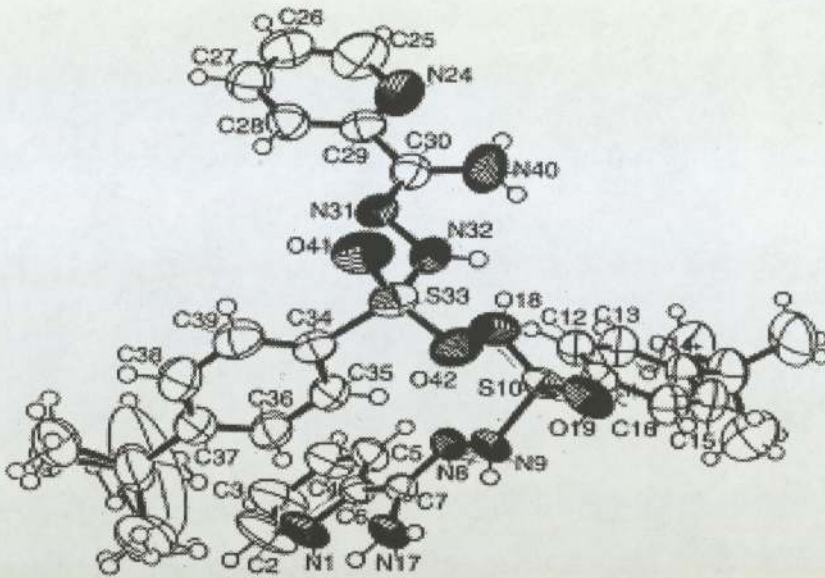
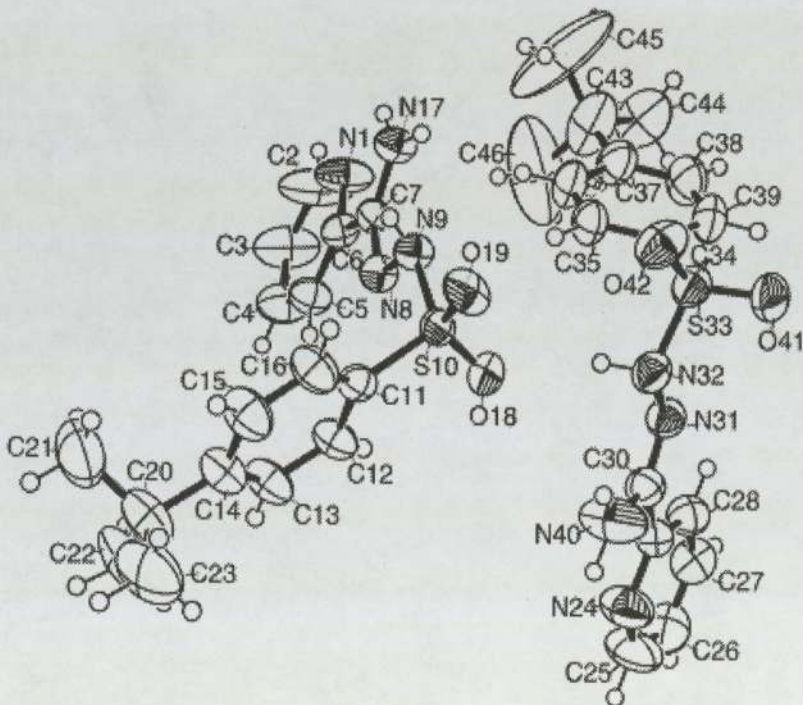


Figure 4. Structure of DLR944

Refinement of the previous data set for DLR944 did not give a credible model for the t-butyl group attached to C37. Even with two positions per methyl group to represent the end points of torsional oscillation, the anisotropic displacement parameters were inconsistent and one was very large. These are obvious in the top panel of **Figure 17** derived from these data.



Old DLR944



Refined DLR944

Figure 17. Crystallography structure of old DLR944 and refined DLR944

After initially unsuccessful attempts a good-sized crystal with smooth regular faces was found, of dimensions 0.5 x 0.45 x 0.40 mm, and used to collect a higher-quality data set.

Refinement of the new data set based on a single position for each atom gives displacement parameters that are never as large as the previous outlier. They provide a more consistent picture of torsional oscillation as a dominant mode of vibration. The smaller vibrational amplitude of C44 can be explained by its location approximately in the plane of the aromatic ring, where it is squeezed against C38 [torsion angle C38-C37-C43-C44 is 11 (1) °], while C45 and C46 being above and below the plane have more freedom to move.

3.6 Comparison between AW464 X-Crystallography and AW464 with MA/MP

Since bond distances are relatively resistant to conformational changes and crystal packing effects, the agreement between bond distances measured by X-ray crystallography and those calculated theoretically can be used to evaluate the quality of the theoretical predictions. Distances involving hydrogen atoms cannot be used in this way since it is difficult to locate them precisely by X-ray methods.

Table 11. Selected experimental and calculated bond distances

Distance Å	X-Ray Crystallography (AW464)	CAChe 3.2 (AW464) with MM3/AM1	CAChe 3.2 (AW464) with MM3/PM3
S1-C2	1.729 (0.002)	1.739	1.798
S1-C7a	1.731 (0.002)	1.688	1.747
C2-N3	1.292 (0.002)	1.322	1.315
N3-C3a	1.396 (0.002)	1.404	1.422
C2-C8	1.528 (0.003)	1.513	1.522
C8-O14	1.420 (0.003)	1.430	1.445
C8-C13	1.494 (0.003)	1.507	1.515
C8-C9	1.498 (0.003)	1.509	1.515
C9-C10	1.319 (0.003)	1.336	1.333
C10-C11	1.464 (0.003)	1.477	1.484
C11-C12	1.457 (0.003)	1.475	1.484
C11-O15	1.224 (0.003)	1.237	1.218
C12-C13	1.316 (0.003)	1.336	1.333

In table 11, MA and MP data are similar to the results from X-ray crystallography, the only significant discrepancies involving S1.

Bond angles also resist deformation due to crystal packing reasonably well, so that comparison is justified.

Table 12. Selected experimental and calculated bond angles

Angle (degrees)	X-Crystallography (AW464)	CHChe 3.2 (AW464) with MM3/AM1	CHChe 3.2 (AW464) with MM3/PM3
C7a-S1-C2	88.61 (0.09)	90.69	89.06
S1-C2-N3	117.21 (0.14)	115.84	114.33
C2-N3-C3a	109.79 (0.16)	109.39	112.10
N3-C3a-C7a	114.64 (0.16)	114.47	113.65
C3a-C7a-S1	109.73 (0.14)	109.60	110.87
S1-C2-C8	119.51 (0.14)	120.05	122.42
N3-C2-C8	123.27 (0.18)	124.11	123.25
C2-C8-O14	105.10 (0.16)	105.75	108.24
C2-C8-C13	108.81 (0.17)	109.68	108.47
C2-C8-C9	107.95 (0.17)	109.02	108.60
C9-C8-O14	110.43 (0.19)	109.32	109.02
C13-C8-O14	111.81 (0.18)	110.33	109.16
C9-C8-C13	112.39 (0.18)	112.52	113.24
C8-C9-C10	123.60 (0.21)	123.30	123.21
C9-C10-C11	121.36 (0.22)	122.24	121.96
C10-C11-C12	117.03 (0.20)	115.55	116.43
C11-C12-C13	121.37 (0.22)	122.38	121.97
C12-C13-C8	123.96 (0.21)	123.26	123.20
C10-C11-O15	121.76 (0.22)	122.02	121.78
C12-C11-O15	121.19 (0.22)	122.43	121.79

In a number of cases MA is better than MP, as shown by the following data picked out from table 12.

S1-C2-N3	117.21 (0.14)	115.84	114.33
C2-N3-C3a	109.79 (0.16)	109.39	112.10
N3-C3a-C7a	114.64 (0.16)	114.47	113.65
C3a-C7a-S1	109.73 (0.14)	109.60	110.87
S1-C2-C8	119.51 (0.14)	120.05	122.42
N3-C2-C8	123.27 (0.18)	124.11	123.25
C2-C8-O14	105.10 (0.16)	105.75	108.24
C2-C8-C13	108.81 (0.17)	109.68	108.47
C9-C8-O14	110.43 (0.19)	109.32	109.02
C13-C8-O14	111.81 (0.18)	110.33	109.16

Torsion angles are not as suitable for use as comparison standards, but instead demonstrate how conformations may change when a molecule is considered on its own, free from the influence of nearby molecules in a crystal.

Table 13. Selected experimental and calculated torsion angles

Torsion angle (degrees)	X-Crystallography (AW464)	CHChe 3.2 (AW464) with MM3/AM1	CHChe 3.2 (AW464) with MM3/PM3
C7a-S1-C2-N3	1.57 (0.17)	0.20	-0.03
S1-C2-N3-C3a	-1.62 (0.23)	-0.17	0.08
C2-N3-C3a-C7a	0.77 (0.25)	0.03	-0.11
N3-C3a-C7a-S1	0.35 (0.22)	0.11	0.08
C3a-C7a-S1-C2	-0.98 (0.15)	0.20	-0.03
S1-C2-C8-O14	9.98 (0.23)	-105.78	-177.66

S1-C2-C8-C13	-109.91 (0.18)	135.26	64.03
S1-C2-C8-C9	127.85 (0.17)	11.65	-59.43
N3-C2-C8-O14	-168.82 (0.19)	73.49	2.45
N3-C2-C8-C9	-50.95 (0.25)	-169.07	120.67
N3-C2-C8-C13	71.29 (0.25)	-45.47	-115.87
C2-C8-C9-C10	114.63 (0.23)	-27.30	26.24
C2-C8-C13-C12	-114.48 (0.26)	-27.59	-26.21
O14-C8-C9-C10	-130.99 (0.22)	-24.38	-69.62
O14-C8-C13-C12	129.89 (0.25)	130.18	-69.70
C8-C9-C10-C11	1.66 (0.34)	-179.50	-0.49
C9-C10-C11-O15	-178.95 (0.22)	-8.92	0.37
C9-C10-C11-C12	2.85 (0.32)	174.65	-0.40
C10-C11-C12-C13	-3.20 (0.34)	174.96	-0.36
C11-C12-C13-C8	-0.96 (0.38)	-178.89	-0.18
C12-C13-C8-C9	5.03 (0.32)	-172.78	-0.02
C13-C8-C9-C10	-5.37 (0.30)	-173.12	-0.04

Throughout this study great attention has been paid to the torsion angle N3-C2-C8-O14, as it indicates the stereochemical relationship between the two ring systems. However, certain torsion angles around the C2-C8 bond are entirely different in Table 14. In the crystal structure the two rings are arranged such that S1 nearly eclipses hydroxyl O14 while N3 is far away [S1-C2-C8-O14 is 9.98 (0.23) ° and N3-C2-C8-O14 is -168.82 (19) °]. This arrangement is probably influenced by crystal packing. For the isolated molecule PM3 nearly interchanges these torsion angles, to -177.66° and 2.45° respectively. This is understandable, as it replaces the eclipsed S1 with the smaller N3, which also is a better acceptor for an intramolecular hydrogen bond from O14-H. It is difficult to see any advantage in

the structure predicted by AM1, where S1 now nearly eclipses C9, S1-C2-C8-C9 being 11.65° . No significant hydrogen bonding is expected, and steric clash may be a problem.

4. Conclusion

On balance the modelling results support a preference for optimization by molecular mechanics followed by PM3. The alternative with AM1 does show some significant advantages: it reproduces the crystallographic bond angles of AW464 better, and its generally lower energy values for the thiol adducts might be interpreted as showing improved stability. However, PM3 provides more satisfying and understandable predictions of torsion angles in AW464. It also predicts that the less crowded down-down Two SCH₃ adduct is more stable than the up-up isomer, unlike AM1. These results influenced the decision by Dr. Rathbone to prefer PM3 for the calculations involving the full thioredoxin molecule.

Calculations on adducts of AW464 with dithiols and with the Cys-Gly-Pro-Cys fragment from thioredoxin have generated a number of structures with satisfactory geometry, energy and appearance. Some of these structures would not be compatible with the remainder of the thioredoxin molecule, but nevertheless this work supports the hypothesis that AW464 can undergo a double Michael addition with thioredoxin.

The improved X-ray data for JMB033 now make it clear that its reactive quinol portion is very similar to AW464. While additional modelling studies will be needed to confirm that its extra steric bulk does not interfere with thioredoxin binding, this appears to be a likely mechanism of action.

The improved X-ray data for DLR944 provide a consistent picture of the t-butyl substituents on the aromatic ring. They are undergoing torsional oscillation, which is particularly large in one molecule, but the amount of oscillation can be understood in terms of the environment of the group.

References

1. Leach, A. R. 2001. *Molecular Modelling Principles and Applications*. Pearson Education Limited, Essex.
2. Flower, D. R. 2002. *Drug Design Cutting Edge Approaches*, The Royal Society of Chemistry, Cambridge.
3. D. B. Boyd, 1990. Successes of computer-assisted molecular design, *Rev. Comput. Chem.* 1: 355-371.
4. M. A. Navia and M.A. Murcko, 1992. Use of structural information in drug design, *curr. Opin. Struct. Biol.* 2: 202-210.
5. J. W. Erickson and S. W. Fesik, 1992. Macromolecular X-ray crystallography and NMR as tools for structure-based drug design, *Annu. Rep. Med. Chem.* 27: 271-289.
6. C. E. Bugg, W. M. Carson, and J. A. Montgomery, 1993. Drugs by design, *Sci. Am.* Dec. 92-98,.
7. R. Peters and R. C. McKinstry, 1994. three-dimensional modelling and drug development: Has rational drug design arrived? *Biotechnology* 12: 147-150.
8. P. J. Whittle and T. L. Blundell, 1994. Protein structure-based drug design: *Annu. Rev. Biophys. Biomol. Struct.* 23: 349-375.
9. W. G. J. Hol and C. L. M. J. Verlinde, 1994. Structure-based drug design: Progress, results, and challenges, *structure* 2: 577-587.
10. J. Greer, J. W. Erickson, J. L. Baldwin, ND m. d. Varney, 1994. Application of the three-dimensional structures of protein target molecules in structure- based drug design, *J. Med. Chem.* 37: 1035-1054.

11. W. C. Guida, 1994. Software for structure-based drug design, *Curr. Opin. Struct. Biol.* 4: 777-781.
12. R. C. Jackson, 1995 Update on computer-aided drug design, *Curr. Opin. Biotechnol.* 6: 646-651.
13. Goodman, J. M. 1998. *Chemical Applications of Molecular Modelling*. The Royal Society of Chemistry, Cambridge.
14. Pople, J. A., Santry, D. P., Segal, G. A. 1965. 'Approximate Self-Consistent Molecular Orbital Theory. I. Invariant Procedures' *J. Chem. Phys.*, 43, S129-S135.
15. Pople, J. A., Segal, G. A. 1965. 'Approximate Self-Consistent Molecular Orbital Theory. II. Calculations with Complete Neglect of Overlap' *J. Chem. Phys.*, 43, S136-S149.
16. Bingham, R. C., Dewar, M. J. S., Lo, D. H. 1975. 'Ground States of Molecules. XXV. MINDO/3. An Improved Version of the MINDO Semi-empirical SCF-MO Method' *J. Am. Chem. Soc.*, 97, 1285-1293
17. Dewar, M. J. S., and Thiel, W. 1977. 'Ground States of Molecules. 38. The MNDO Method. Approximations and Parameters' *J. Am. Chem. Soc.*, 99, 4899-4907.
18. Dewar, M. J. S., Zoebisch, E. G., Healy, E. F., Stewart, J. J. P. 1985. 'AM1: A New General Purpose Quantum Mechanical Molecular Model' *J. Am. Chem. Soc.*, 107, 3902-3909.
19. Stewart, J. J. P. 1989. 'Optimization of Parameters for Semiempirical Methods. I. Method' *J. Comp. Chem.*, 10, 209-220.
20. Stewart, J. J. P. 1990. 'MOPAC: A Semi-empirical Molecular Orbital Program' *J. Comp. -Aided Mol. Des.*, 4, 1-105

21. Pople, J. A. 1975. Some Deficiencies of MINDO/3 Semiempirical Theory, McGraw Hill, New York.
22. Dewar, M. J. S., Jie, C., Yu, J. 1993. SAM1, The First of A New Series of General Purpose Quantum Mechanical Molecular Models' *Tetrahedron* 49, 5003-5038.
23. O. Ermer, 1976. Calculation of molecular properties using force field. Applications in organic chemistry, *Struct. Bonding (Berlin)* 27: 161.
24. C. L. Altona and D. H. Faber, 1974. Empirical force field calculations. A tool in structural organic chemistry, *Top. Curr. Chem.* 45: 1.
25. E. M. Engler, J. D. Andose, and P. v. R. Schleyer, 1973. Critical evaluation of molecular mechanics, *J. Am. Chem. Soc.* 95: 8005.
26. L. S. Bartell, 1977. Representations of molecular force fields, 3. On gauche conformational energy, *J. Am. Chem. Soc.* 99: 3279.
27. D. N. J. White and M. Bovill, 1977. Molecular mechanics calculations on alkanes and nonconjugated alkenes, *J. Chem. Soc. Perkin. Trans. 2:* 1610.
28. J. D. Dunitz and H. B. Burgi, 1975. Non-bonded interactions in organic molecules. *International Review of Science: Physical Chemistry, Series Two, 1975-1976 Vol. II* (A. D. Buckingham and J. M. Robertson, eds.) , Butterworths, London, p. 81.
29. S. R. Niketic and K. Rasmussen, 1977. *The Consistent Force Field*, Springer, New York.
30. A. Warshel, 1977. The consistent force field and its quantum mechanical extension, *Semi-empirical Methods of Electronic Structure Calculation Vol. 7* (G. A. Segal, ed.), Plenum, New York, P. 133.

31. D. N. J. White, 1978. Molecular mechanics calculations, *Mol. Struct. Diiffr. Methods* 6:38.
32. K. Mislow, D. A. Dougherty, and W. D. Hounshell, 1978. Some applications of the empirical force field method to stereochemistry, *Bull. Soc. Chem. Belg.* 87: 555.
33. J. E. Williams, P. J. Stang, and P. v. R. Schleyer, 1968. Physical organic chemistry: Quantitative conformational analysis; calculation methods, *Annu. Rev. Phys. Chem.* 19: 531.
34. U. Dinur and A. T. Hagler, 1991. New approaches to empirical force field, *Reviews in Computational chemistry Vol. 2* (K. Lipkowitz and D. Boyd, eds.), VCH, New York, pp, 99-184.
35. J. B. Hendrickson, 1961. Molecular geometry. I. Machine computation of the common rings, *J. Am. Chem. Soc.* 83: 4537.
36. S. Lifson and A. Warshel, 1968. Consistent force field calculations of conformations, vibrational spectra, and enthalpies of cycloalkane and n-alkane molecules, *J. Chem. Phys.* 49:: 5116.
37. O. Ermer and S. Lifson, 1973. Consistent force field calculations. III. Vibrations, conformations, and heats of hydrogenation of nonconjugated olefins, *J. Am. Chem. Soc.* 95: 4121.
38. N. L. Allinger and J. T. Sprague, 1973. The calculation of the structures of hydrocarbons containing delocalized electronic systems by the molecular mechanics method, *J. Am. Chem. Soc.* 95: 3893.
39. K. B. Wiberg, 1965. A scheme for strain energy minimization. Application to the cycloalkanes, *J. Am. Chem. Soc.* 87: 1070.
40. Allinger N. L. 1977. *Conformational Analysis* 130. MM2. A

Hydrocarbon Force Field Utilizing V1 and V2d Torsional Terms. *J. Am. Chem. Soc.* 99: 8127-8134.

41. Allinger N. L., Chen, K. and Lii, J-H. 1996a. An Improved Force Field (MM4) for Saturated Hydrocarbons. *Journal of Computational Chemistry* 17:642-668.
42. Allinger N. L., Chen, K., Katzenelenbogen, J. A., Wilson, S. R. and Anstead, G. M. 1996b. Hyperconjugative Effects on Carbon-Carbon Bond Lengths in Molecular Mechanics (MM4). *Journal of Computational Chemistry* 17:747-755.
43. Allinger N. L., Li, F. and Yan, L. 1990a. Molecular Mechanics. The MM3 Force Field for Alkenes. *Journal of Computational Chemistry* 11:848-867.
44. Allinger N. L., Li, F., Yan, L. and Tai, J. C. 1990b. Molecular Mechanics (MM3) Calculations on Conjugated Hydrocarbons. *Journal of Computational Chemistry* 11:868-895.
45. Allinger N. L., Yuh, Y. H. and Lii, J-J. 1989. Molecular Mechanics. The MM3 Force Field for Hydrocarbons. *J. Am. Chem. Soc.* 111:8551-9556.
46. Lii, J-H. and Allinger, N. L. 1989. Molecular Mechanics. The MM3 Force Field for Hydrocarbons. 2 Vibrational Frequencies and Thermodynamics. *J. Am. Chem. Soc.* 111: 8556-8582.
47. Nevins, N., Chen, K. and Allinger, N. L. 1996a. Molecular Mechanics (MM4) Calculations on Alkenes. *Journal of Computational Chemistry* 17: 669-694.
48. Nevins, N., Chen, K. and Allinger, N. L. 1996b. Molecular Mechanics (MM4) Calculations on Conjugated Hydrocarbons. *Journal of*

Computational Chemistry 17: 659-729.

49. Nevins, N., Chen, K. and Allinger, N. L. 1996c. Molecular Mechanics (MM4) Vibrational Frequency Calculations for Alkenes and Conjugated Hydrocarbons. *Journal of Computational Chemistry* 17:730-746.
50. Weiner S J, Kollman, P. A., Case, D. A., Singh, U. C., Ghio, C., Alagona, G., Profeta, S. and Weiner, P. 1984. A New Force Field for Molecular Mechanical Simulation of Nucleic Acids and Proteins. *J. Am. Chem. Soc.* 106:765-784.
51. Cornell, W. D., Cieplak, P., Bayly, C. I., Gould, I. R., Merz, K. M. Jr, Ferguson, D. M., Spellmeyer, D. C., Fox, T., Caldwell, J. W. and Kollman, P. A. 1995. A Second Generation Force Field for the Simulation of Proteins, Nucleic Acids and Organic Molecules. *J. Am. Chem. Soc.* 117: 5179-5197.
52. Schwalbe, C. H., Lowe, P. R. and Stevens, M. F. G. 2002. Geometry and hydrogen bonding in two anti-cancer benzothiazoles. *Journal of Pharmacy and Pharmacology* 54 (Suppl.): S-69.
53. Weichsel, A., Gasdaska, J. R., Powis, G., Montfort, W. R 1996 Crystal Structures of Reduced, Oxidized, and Mutated Human Thioredoxins: Evidence for a Regulatory Homodimer. *Structure* 4:735.
54. Wells, G., Berry, J. M., Bradshaw, T. D., Burger, A. M., Seaton, A., Wang, B., Westwell, A. D., Stevens, M. F. G. 2003 4-Substituted 4-Hydroxycyclohexa-2,5-dien-1-ones with Selective Activities against Colon and Renal Cancer Cell Lines. *J. Med. Chem.* 46: 532-541.
55. Kunkel, M. W., Kirkpatrick, D.L, Johnson, J. L. and Powis, G. 1997

Cell Line-directed Screening Assay for Inhibitors of Thioredoxin
Reductase Signaling as Potential Anti-cancer Drugs. *Anti-Cancer Drug
Des.*, 12: 659-670

56. Morrison, R. T. 1992 *Organic Chemistry*. Prentice Hall, Englewood
Cliffs, NJ.

Appendices

Appendix 1. Results of a Cambridge Structural Database search for cyclohexadienone derivatives in which the sp^3 tetrahedral bridgehead carbon atom is bonded to one C and one O atom, neither of which is part of a ring. With respect to the reference plane defined by the two C=C groups DISTC is the deviation (\AA) of the attached C atom and DISTO is for the corresponding oxygen atom.

Refcode	DISTC	DISTO
DEZTIL	1.303	0.992
FOHHEP	1.534	0.785
JEXKOM	1.626	0.695
QEQMII	1.632	0.719
RIPBEX	1.762	0.501
SAXMEJ	1.339	1.030
SCQUCO	1.800	0.509
SIPJOQ	1.377	0.983
VOLBED	1.364	0.964
VUWYIV	1.706	0.541
XAYDEG	1.127	1.204
XAYDEG	1.248	1.093
ZAVPAN	1.403	0.962

Appendix 2. Crystallographic results for compound BW114 from
crystal sample JMB033.

Table 1. Crystal data and structure refinement

Identification code	jmb33re
Empirical formula	C ₂₀ H ₁₅ N O ₄ S
Formula weight	365.39
Temperature	293(2) K
Wavelength	0.71073 Å
Crystal system	Monoclinic
Space group	P2 ₁ /c
Unit cell dimensions	a = 15.996(4) Å alpha = 90 deg. b = 13.457(2) Å beta = 99.21(2) deg. c = 15.769(4) Å gamma = 90 deg.
Volume	3350.6(13) Å ³
Z	8
Density (calculated)	1.449 Mg/m ³
Absorption coefficient	0.220 mm ⁻¹
F(000)	1520
Crystal size	0.5 x 0.4 x 0.3 mm
Theta range for data collection	2.00 to 25.02 deg.
Index ranges	-19 ≤ h ≤ 0, -15 ≤ k ≤ 15, -18 ≤ l ≤ 18
Reflections collected	12124 by omega-2theta scans
Independent reflections	6007 [R(int) = 0.0512], 1979 with F ≤ 4σ
Structure solution	Direct methods: SHELXS
Refinement method	Full-matrix least-squares on F ² : SHELXL
Data / restraints / parameters	6007 / 0 / 472
Goodness-of-fit on F ²	1.096
Final R indices [I > 2σ(I)]	R ₁ = 0.0624, wR ₂ = 0.1597
R indices (all data)	R ₁ = 0.1112, wR ₂ = 0.1940

Largest diff. peak and hole 1.107 and -0.426 e.A⁻³. Two peaks that exceed 1 e.A⁻³ are related to the sulfur atoms by the pseudo-operation $\pm 1/2+x, 3/2-y, z$ arising from the combination of space group symmetry and the twin law which interchanges x and z. With the a and c axes nearly equal the crystals are subject to non-merohedral twinning which leads to complete overlap of reflections at low angles but resolution at high angles. Compensation with a single parameter under-corrects the low-angle reflections, which contribute to these peaks. The third highest peak is 0.46 e.A⁻³.

Table 2. Atomic coordinates ($\times 10^4$) and equivalent isotropic displacement parameters ($\text{\AA}^2 \times 10^3$) for jmb33re. $U(\text{eq})$ is defined as one third of the trace of the orthogonalized U_{ij} tensor.

	x	y	z	$U(\text{eq})$
N(1)	9690 (2)	9499 (2)	2153 (2)	37 (1)
C(2)	9534 (3)	10078 (3)	1384 (3)	37 (1)
C(3)	10204 (3)	10676 (3)	1367 (3)	45 (1)
C(3A)	10830 (3)	10492 (3)	2103 (3)	45 (1)
C(4)	11631 (3)	10917 (3)	2387 (4)	61 (1)
C(5)	12075 (3)	10609 (4)	3159 (4)	67 (2)
C(6)	11739 (3)	9908 (4)	3648 (4)	66 (1)
C(7)	10957 (3)	9472 (4)	3385 (3)	54 (1)
C(7A)	10510 (3)	9774 (3)	2598 (3)	42 (1)
C(8)	8720 (3)	10110 (3)	748 (3)	40 (1)
C(9)	7991 (3)	10391 (3)	1197 (3)	42 (1)
C(10)	7537 (3)	11214 (3)	1031 (3)	47 (1)
C(11)	7704 (3)	11913 (3)	363 (3)	54 (1)
C(12)	8354 (3)	11633 (3)	-130 (3)	53 (1)
C(13)	8819 (3)	10842 (3)	51 (3)	50 (1)

O(14)	8585 (2)	9173 (2)	310 (2)	54 (1)
O(15)	7272 (3)	12667 (3)	205 (3)	83 (1)
S(16)	9294 (1)	8371 (1)	2317 (1)	39 (1)
O(17)	8425 (2)	8377 (2)	1928 (2)	46 (1)
O(18)	9502 (2)	8196 (2)	3213 (2)	54 (1)
C(19)	9856 (3)	7525 (3)	1774 (3)	39 (1)
C(20)	10653 (3)	7196 (3)	2149 (3)	46 (1)
C(21)	11074 (3)	6520 (3)	1725 (3)	53 (1)
C(22)	10713 (3)	6159 (3)	928 (3)	54 (1)
C(23)	9922 (3)	6472 (3)	566 (3)	61 (1)
C(24)	9487 (3)	7162 (3)	980 (3)	49 (1)
N(1')	4613 (2)	5234 (2)	2124 (2)	36 (1)
C(2')	3814 (3)	4722 (3)	1984 (3)	38 (1)
C(3')	3760 (3)	4158 (3)	2675 (3)	44 (1)
C(3A')	4503 (3)	4291 (3)	3307 (3)	44 (1)
C(4')	4756 (4)	3868 (3)	4110 (3)	57 (1)
C(5')	5543 (4)	4122 (4)	4554 (3)	62 (1)
C(6')	6056 (4)	4774 (4)	4211 (3)	66 (1)
C(7')	5831 (3)	5203 (3)	3409 (3)	53 (1)
C(7A')	5032 (3)	4947 (3)	2966 (3)	41 (1)

C(8')	3216 (3)	4677 (3)	1130 (3)	40 (1)
C(9')	2510 (3)	3957 (3)	1221 (3)	49 (1)
C(10')	2379 (3)	3117 (4)	787 (3)	54 (1)
C(11')	2925 (3)	2806 (4)	184 (3)	56 (1)
C(12')	3570 (3)	3509 (3)	6 (3)	49 (1)
C(13')	3697 (3)	4356 (3)	430 (3)	47 (1)
O(14')	2769 (2)	5593 (2)	915 (2)	56 (1)
O(15')	2843 (3)	2000 (3)	-194 (3)	89 (1)
S(16')	4801 (1)	6360 (1)	1752 (1)	39 (1)
O(17')	4387 (2)	6396 (2)	880 (2)	49 (1)
O(18')	5695 (2)	6491 (2)	1929 (2)	51 (1)
C(19')	4320 (3)	7209 (3)	2367 (3)	40 (1)
C(20')	4719 (3)	7465 (3)	3180 (3)	50 (1)
C(21')	4340 (3)	8114 (4)	3658 (3)	61 (1)
C(22')	3577 (3)	8541 (3)	3324 (3)	60 (1)
C(23')	3187 (3)	8299 (4)	2513 (4)	63 (1)
C(24')	3547 (3)	7621 (3)	2025 (3)	52 (1)

Table 3. Bond lengths [Å] and angles [deg] for jmb33re.

N(1) - C(2)	1.430 (5)
N(1) - C(7A)	1.434 (5)
N(1) - S(16)	1.680 (3)
C(2) - C(3)	1.345 (6)
C(2) - C(8)	1.512 (6)
C(3) - C(3A)	1.428 (6)
C(3A) - C(7A)	1.389 (6)
C(3A) - C(4)	1.409 (6)
C(4) - C(5)	1.372 (8)
C(5) - C(6)	1.380 (8)
C(6) - C(7)	1.384 (7)
C(7) - C(7A)	1.390 (6)
C(8) - O(14)	1.437 (5)
C(8) - C(13)	1.503 (6)
C(8) - C(9)	1.506 (6)
C(9) - C(10)	1.328 (6)
C(10) - C(11)	1.469 (6)

C(11)-O(15)	1.230 (5)
C(11)-C(12)	1.445 (7)
C(12)-C(13)	1.303 (6)
S(16)-O(18)	1.419 (3)
S(16)-O(17)	1.428 (3)
S(16)-C(19)	1.756 (4)
C(19)-C(24)	1.386 (6)
C(19)-C(20)	1.389 (6)
C(20)-C(21)	1.368 (6)
C(21)-C(22)	1.384 (7)
C(22)-C(23)	1.369 (7)
C(23)-C(24)	1.385 (6)
N(1')-C(2')	1.438 (5)
N(1')-C(7A')	1.442 (5)
N(1')-S(16')	1.670 (3)
C(2')-C(3')	1.342 (6)
C(2')-C(8')	1.523 (6)
C(3')-C(3A')	1.434 (6)
C(3A')-C(4')	1.387 (6)
C(3A')-C(7A')	1.390 (6)

C(4')-C(5')	1.382 (7)
C(5')-C(6')	1.371 (8)
C(6')-C(7')	1.384 (7)
C(7')-C(7A')	1.397 (6)
C(8')-O(14')	1.438 (5)
C(8')-C(13')	1.506 (6)
C(8')-C(9')	1.512 (6)
C(9')-C(10')	1.321 (7)
C(10')-C(11')	1.452 (7)
C(11')-O(15')	1.234 (6)
C(11')-C(12')	1.460 (7)
C(12')-C(13')	1.321 (6)
S(16')-O(18')	1.423 (3)
S(16')-O(17')	1.427 (3)
S(16')-C(19')	1.755 (4)
C(19')-C(20')	1.380 (6)
C(19')-C(24')	1.383 (6)
C(20')-C(21')	1.359 (7)
C(21')-C(22')	1.375 (7)
C(22')-C(23')	1.370 (7)

C(23') - C(24')	1.378 (7)
C(2) - N(1) - C(7A)	107.2 (3)
C(2) - N(1) - S(16)	127.1 (3)
C(7A) - N(1) - S(16)	119.8 (3)
C(3) - C(2) - N(1)	108.1 (4)
C(3) - C(2) - C(8)	125.1 (4)
N(1) - C(2) - C(8)	126.4 (3)
C(2) - C(3) - C(3A)	109.7 (4)
C(7A) - C(3A) - C(4)	120.1 (4)
C(7A) - C(3A) - C(3)	107.7 (4)
C(4) - C(3A) - C(3)	132.1 (4)
C(5) - C(4) - C(3A)	118.3 (5)
C(4) - C(5) - C(6)	120.6 (5)
C(5) - C(6) - C(7)	122.5 (5)
C(6) - C(7) - C(7A)	117.0 (5)
C(7) - C(7A) - C(3A)	121.5 (4)
C(7) - C(7A) - N(1)	131.3 (4)
C(3A) - C(7A) - N(1)	107.2 (4)
O(14) - C(8) - C(13)	104.4 (3)

O(14)-C(8)-C(9)	112.3(3)
C(13)-C(8)-C(9)	111.0(3)
O(14)-C(8)-C(2)	110.0(3)
C(13)-C(8)-C(2)	108.9(3)
C(9)-C(8)-C(2)	110.1(3)
C(10)-C(9)-C(8)	123.9(4)
C(9)-C(10)-C(11)	121.3(4)
O(15)-C(11)-C(12)	122.3(5)
O(15)-C(11)-C(10)	120.9(5)
C(12)-C(11)-C(10)	116.7(4)
C(13)-C(12)-C(11)	121.9(4)
C(12)-C(13)-C(8)	125.0(4)
O(18)-S(16)-O(17)	118.97(19)
O(18)-S(16)-N(1)	105.59(18)
O(17)-S(16)-N(1)	107.10(17)
O(18)-S(16)-C(19)	108.75(19)
O(17)-S(16)-C(19)	109.56(19)
N(1)-S(16)-C(19)	106.07(17)
C(24)-C(19)-C(20)	120.2(4)
C(24)-C(19)-S(16)	119.4(3)

C(20) - C(19) - S(16)	120.4 (3)
C(21) - C(20) - C(19)	119.6 (4)
C(20) - C(21) - C(22)	120.7 (4)
C(23) - C(22) - C(21)	119.6 (4)
C(22) - C(23) - C(24)	120.7 (5)
C(19) - C(24) - C(23)	119.2 (4)
C(2') - N(1') - C(7A')	106.5 (3)
C(2') - N(1') - S(16')	125.9 (3)
C(7A') - N(1') - S(16')	118.9 (3)
C(3') - C(2') - N(1')	108.5 (3)
C(3') - C(2') - C(8')	125.7 (4)
N(1') - C(2') - C(8')	124.8 (3)
C(2') - C(3') - C(3A')	109.9 (4)
C(4') - C(3A') - C(7A')	120.4 (4)
C(4') - C(3A') - C(3')	132.2 (4)
C(7A') - C(3A') - C(3')	107.4 (4)
C(5') - C(4') - C(3A')	118.1 (5)
C(6') - C(5') - C(4')	120.8 (5)
C(5') - C(6') - C(7')	122.9 (5)
C(6') - C(7') - C(7A')	115.8 (5)

C(3A')-C(7A')-C(7')	121.9(4)
C(3A')-C(7A')-N(1')	107.7(4)
C(7')-C(7A')-N(1')	130.3(4)
O(14')-C(8')-C(13')	111.5(3)
O(14')-C(8')-C(9')	102.8(3)
C(13')-C(8')-C(9')	111.3(4)
O(14')-C(8')-C(2')	113.1(3)
C(13')-C(8')-C(2')	109.7(3)
C(9')-C(8')-C(2')	108.3(3)
C(10')-C(9')-C(8')	123.9(4)
C(9')-C(10')-C(11')	121.6(4)
O(15')-C(11')-C(10')	122.8(5)
O(15')-C(11')-C(12')	120.0(5)
C(10')-C(11')-C(12')	117.2(4)
C(13')-C(12')-C(11')	121.2(4)
C(12')-C(13')-C(8')	124.3(4)
O(18')-S(16')-O(17')	118.77(19)
O(18')-S(16')-N(1')	105.91(17)
O(17')-S(16')-N(1')	106.73(17)
O(18')-S(16')-C(19')	109.06(19)

O(17')-S(16')-C(19')	109.49(19)
N(1')-S(16')-C(19')	106.10(18)
C(20')-C(19')-C(24')	120.9(4)
C(20')-C(19')-S(16')	119.8(3)
C(24')-C(19')-S(16')	119.3(3)
C(21')-C(20')-C(19')	119.7(4)
C(20')-C(21')-C(22')	120.2(5)
C(23')-C(22')-C(21')	120.2(5)
C(22')-C(23')-C(24')	120.6(5)
C(23')-C(24')-C(19')	118.4(4)

Table 4. Anisotropic displacement parameters ($\text{\AA}^2 \times 10^3$) for jmb33re. The anisotropic displacement factor exponent takes the form:

$$-2 \pi^2 [h^2 a^{*2} U_{11} + \dots + 2 h k a^* b^* U_{12}]$$

	U11	U22	U33	U23	U13	U12
N(1)	41 (2)	27 (2)	43 (2)	0 (1)	3 (1)	-2 (1)
C(2)	45 (2)	26 (2)	42 (2)	-3 (2)	10 (2)	-1 (2)
C(3)	48 (3)	33 (2)	54 (3)	-1 (2)	9 (2)	-2 (2)
C(3A)	42 (2)	32 (2)	59 (3)	-9 (2)	4 (2)	1 (2)
C(4)	42 (3)	44 (3)	94 (4)	-8 (2)	6 (3)	-4 (2)
C(5)	39 (3)	64 (3)	91 (4)	-19 (3)	-10 (3)	5 (2)
C(6)	59 (3)	66 (3)	65 (3)	-16 (3)	-11 (3)	17 (3)
C(7)	50 (3)	58 (3)	50 (3)	-3 (2)	-6 (2)	5 (2)
C(7A)	39 (2)	37 (2)	51 (2)	-14 (2)	7 (2)	4 (2)
C(8)	46 (2)	30 (2)	44 (2)	-5 (2)	7 (2)	-6 (2)
C(9)	42 (2)	41 (2)	40 (2)	6 (2)	2 (2)	-5 (2)
C(10)	40 (2)	57 (3)	44 (2)	0 (2)	2 (2)	9 (2)
C(11)	63 (3)	39 (2)	51 (3)	6 (2)	-15 (2)	6 (2)
C(12)	63 (3)	49 (3)	47 (3)	10 (2)	5 (2)	-7 (2)

C(13)	55(3)	48(3)	45(2)	1(2)	9(2)	-8(2)
O(14)	72(2)	37(2)	54(2)	-13(1)	11(2)	-14(1)
O(15)	103(3)	60(2)	84(3)	25(2)	6(2)	35(2)
S(16)	42(1)	32(1)	44(1)	4(1)	11(1)	2(1)
O(17)	36(2)	37(2)	67(2)	6(1)	11(1)	0(1)
O(18)	67(2)	53(2)	44(2)	9(1)	15(2)	4(2)
C(19)	41(2)	24(2)	53(2)	5(2)	14(2)	0(2)
C(20)	50(3)	39(2)	47(2)	8(2)	3(2)	8(2)
C(21)	50(3)	43(2)	67(3)	10(2)	10(2)	16(2)
C(22)	66(3)	37(2)	64(3)	0(2)	21(2)	11(2)
C(23)	69(3)	46(3)	67(3)	-14(2)	8(3)	5(2)
C(24)	46(3)	38(2)	59(3)	-8(2)	-1(2)	4(2)
N(1')	43(2)	29(2)	35(2)	5(1)	2(1)	1(1)
C(2')	40(2)	33(2)	42(2)	0(2)	8(2)	2(2)
C(3')	51(3)	36(2)	47(2)	-1(2)	15(2)	-4(2)
C(3A')	61(3)	30(2)	39(2)	-2(2)	6(2)	7(2)
C(4')	91(4)	39(2)	43(3)	7(2)	14(2)	6(2)
C(5')	86(4)	48(3)	47(3)	3(2)	-5(3)	15(3)
C(6')	72(4)	50(3)	66(3)	1(2)	-15(3)	10(2)

C(7')	53 (3)	42 (2)	58 (3)	5 (2)	-7 (2)	2 (2)
C(7A')	49 (2)	31 (2)	43 (2)	1 (2)	3 (2)	8 (2)
C(8')	41 (2)	34 (2)	43 (2)	3 (2)	3 (2)	1 (2)
C(9')	37 (2)	57 (3)	51 (3)	6 (2)	6 (2)	-2 (2)
C(10')	41 (3)	56 (3)	61 (3)	8 (2)	-4 (2)	-13 (2)
C(11')	42 (3)	50 (3)	71 (3)	-10 (2)	-9 (2)	-2 (2)
C(12')	43 (2)	56 (3)	49 (3)	-12 (2)	8 (2)	-1 (2)
C(13')	41 (2)	51 (3)	47 (2)	6 (2)	5 (2)	-8 (2)
O(14')	50 (2)	48 (2)	68 (2)	12 (2)	3 (2)	11 (1)
O(15')	74 (3)	67 (2)	124 (4)	-43 (2)	11 (2)	-21 (2)
S(16')	45 (1)	32 (1)	42 (1)	5 (1)	9 (1)	-1 (1)
O(17')	70 (2)	39 (2)	37 (2)	6 (1)	7 (1)	-2 (1)
O(18')	43 (2)	49 (2)	62 (2)	5 (1)	12 (1)	-6 (1)
C(19')	44 (2)	32 (2)	42 (2)	2 (2)	5 (2)	-3 (2)
C(20')	49 (3)	51 (3)	47 (3)	-5 (2)	1 (2)	-1 (2)
C(21')	68 (3)	59 (3)	55 (3)	-16 (2)	7 (2)	-4 (2)
C(22')	67 (3)	44 (3)	70 (3)	-15 (2)	20 (3)	1 (2)
C(23')	58 (3)	53 (3)	77 (4)	-4 (3)	7 (3)	13 (2)
C(24')	58 (3)	41 (2)	54 (3)	-3 (2)	1 (2)	6 (2)

Table 5. Hydrogen coordinates ($\times 10^4$) and isotropic displacement parameters ($\text{\AA}^2 \times 10^3$) for jmb33re.

U(eq)	x	y	z	
H(3)	10253	11140	941	54
H(4)	11853	11395	2059	73
H(5)	12608	10875	3356	80
H(6)	12050	9722	4173	79
H(7)	10740	8997	3720	65
H(9)	7852	9963	1616	50
H(10)	7104	11350	1344	57
H(12)	8444	12029	-590	64
H(13)	9243	10722	-275	59
H(14)	8094	8994	303	81
H(20)	10899	7433	2685	55
H(21)	11609	6302	1974	64
H(22)	11007	5706	640	65
H(23)	9674	6218	36	73
H(24)	8952	7379	727	58
H(3')	3308	3743	2736	53

H(4')	4407	3427	4342	69
H(5')	5726	3848	5093	74
H(6')	6578	4935	4531	79
H(7')	6189	5635	3178	63
H(9')	2147	4114	1607	58
H(10')	1925	2716	869	65
H(12')	3897	3358	-414	59
H(13')	4111	4782	287	56
H(14')	3084	5993	734	84
H(20')	5244	7194	3398	60
H(21')	4598	8271	4213	73
H(22')	3326	8995	3649	72
H(23')	2673	8595	2289	76
H(24')	3277	7445	1479	63

Appendix 3. Crystallographic results for compound DLR944 from
crystal sample DR944RFR.

Table 1. Crystal data and structure refinement for dr944rfr.

Identification code	dr944rfr
Empirical formula	C32 H40 N8 O4 S2
Formula weight	664.84
Temperature	293(2) K
Wavelength	0.71073 A
Crystal system	Monoclinic
Space group	P21/c
Unit cell dimensions	a = 11.062(2) A alpha = 90 deg. b = 16.2625(16) A beta = 105.027(11) deg. c = 20.224(2) A gamma = 90 deg.
Volume	3513.9(8) A ³
Z	4
Density (calculated)	1.257 Mg/m ³
Absorption coefficient	0.198 mm ⁻¹
F(000)	1408
Crystal size	0.50 x 0.45 x 0.40 mm
Theta range for data collection	2.09 to 25.04 deg.
Index ranges	-12<=h<=13, -19<=k<=0, -24<=l<=2
Reflections collected	6671
Independent reflections	6001 [R(int) = 0.0234]
Refinement method	Full-matrix least-squares on F ²
Data / restraints / parameters	6001 / 0 / 439
Goodness-of-fit on F ²	0.951
Final R indices [I>2sigma(I)]	R1 = 0.0577, wR2 = 0.1730
R indices (all data)	R1 = 0.1012, wR2 = 0.2123
Largest diff. peak and hole	0.527 and -0.363 e.A ⁻³

Table 2. Atomic coordinates ($\times 10^4$) and equivalent isotropic displacement parameters ($\text{\AA}^2 \times 10^3$) for dr944rfr. $U(\text{eq})$ is defined as one third of the trace of the orthogonalized U_{ij} tensor.

	x	y	z	$U(\text{eq})$
N(1)	311 (3)	5613 (3)	918 (2)	77 (1)
C(2)	-561 (4)	5805 (5)	1235 (3)	118 (3)
C(3)	-392 (4)	6320 (5)	1775 (3)	103 (2)
C(4)	763 (4)	6681 (3)	2025 (2)	76 (1)
C(5)	1688 (4)	6492 (3)	1711 (2)	56 (1)
C(6)	1427 (3)	5970 (2)	1157 (2)	45 (1)
C(7)	2370 (3)	5747 (2)	788 (2)	39 (1)
N(8)	3502 (2)	5992 (2)	1058 (2)	44 (1)
N(9)	4318 (2)	5734 (2)	653 (2)	44 (1)
S(10)	5796 (1)	5877 (1)	1023 (1)	44 (1)
C(11)	6056 (3)	6920 (2)	1211 (2)	44 (1)
C(12)	5912 (4)	7224 (2)	1821 (2)	53 (1)
C(13)	6070 (4)	8058 (3)	1955 (2)	63 (1)
C(14)	6389 (4)	8592 (3)	1500 (2)	62 (1)
C(15)	6556 (5)	8257 (3)	897 (2)	71 (1)
C(16)	6384 (4)	7437 (3)	747 (2)	62 (1)

N(17)	1976 (3)	5302 (2)	214 (2)	50 (1)
O(18)	6083 (3)	5432 (2)	1648 (2)	64 (1)
O(19)	6407 (2)	5658 (2)	506 (2)	63 (1)
C(20)	6547 (5)	9519 (3)	1624 (3)	84 (2)
C(21)	5717 (7)	9982 (4)	994 (3)	113 (2)
C(22)	6098 (8)	9786 (3)	2244 (3)	124 (3)
C(23)	7862 (7)	9762 (4)	1665 (4)	124 (2)
N(24)	8312 (5)	4483 (3)	4176 (2)	88 (1)
C(25)	8282 (7)	4402 (4)	4819 (3)	104 (2)
C(26)	7667 (5)	3780 (4)	5055 (3)	85 (2)
C(27)	7054 (4)	3213 (3)	4596 (2)	71 (1)
C(28)	7076 (4)	3285 (3)	3930 (2)	61 (1)
C(29)	7699 (4)	3921 (2)	3728 (2)	56 (1)
C(30)	7741 (4)	4037 (2)	3007 (2)	54 (1)
N(31)	7081 (3)	3556 (2)	2555 (2)	52 (1)
N(32)	7182 (3)	3753 (2)	1886 (2)	55 (1)
S(33)	6590 (1)	3056 (1)	1310 (1)	54 (1)
C(34)	5005 (4)	2912 (2)	1284 (2)	50 (1)

C(35)	4180 (4)	3548 (2)	1096 (2)	58 (1)
C(36)	2932 (4)	3413 (3)	1035 (2)	65 (1)
C(37)	2459 (4)	2657 (3)	1157 (3)	70 (1)
C(38)	3328 (5)	2024 (3)	1347 (3)	78 (1)
C(39)	4582 (4)	2150 (3)	1417 (2)	68 (1)
N(40)	8463 (5)	4657 (3)	2895 (3)	103 (2)
O(41)	7234 (3)	2306 (2)	1510 (2)	73 (1)
O(42)	6643 (3)	3434 (2)	679 (1)	73 (1)
C(43)	1074 (5)	2551 (4)	1080 (4)	115 (3)
C(44)	746 (6)	1749 (4)	1352 (4)	111 (2)
C(45)	375 (8)	2706 (9)	377 (6)	285 (10)
C(46)	657 (8)	3210 (6)	1560 (8)	252 (8)

Table 3. Bond lengths [Å] and angles [deg] for dr944rfr.

N(1)-C(2)	1.327(6)
N(1)-C(6)	1.337(5)
C(2)-C(3)	1.349(7)
C(2)-H(2)	0.9300
C(3)-C(4)	1.378(7)
C(3)-H(3)	0.9300
C(4)-C(5)	1.373(6)
C(4)-H(4)	0.9300
C(5)-C(6)	1.374(5)
C(5)-H(5)	0.9300
C(6)-C(7)	1.477(5)
C(7)-N(8)	1.293(4)
C(7)-N(17)	1.341(5)
N(8)-N(9)	1.429(4)
N(9)-S(10)	1.628(3)
N(9)-H(9)	0.86(4)
S(10)-O(18)	1.419(3)

S(10) - O(19)	1.431 (3)
S(10) - C(11)	1.745 (4)
C(11) - C(12)	1.377 (5)
C(11) - C(16)	1.376 (5)
C(12) - C(13)	1.386 (6)
C(12) - H(12)	0.9300
C(13) - C(14)	1.376 (6)
C(13) - H(13)	0.9300
C(14) - C(15)	1.390 (6)
C(14) - C(20)	1.532 (6)
C(15) - C(16)	1.370 (6)
C(15) - H(15)	0.9300
C(16) - H(16)	0.9300
N(17) - H(17A)	0.94 (4)
N(17) - H(17B)	0.79 (6)
C(20) - C(23)	1.489 (8)
C(20) - C(22)	1.526 (8)
C(20) - C(21)	1.558 (9)

C (21) -H (21A)	0.9600
C (21) -H (21B)	0.9600
C (21) -H (21C)	0.9600
C (22) -H (22A)	0.9600
C (22) -H (22B)	0.9600
C (22) -H (22C)	0.9600
C (23) -H (23A)	0.9600
C (23) -H (23B)	0.9600
C (23) -H (23C)	0.9600
N (24) -C (25)	1.314 (7)
N (24) -C (29)	1.341 (5)
C (25) -C (26)	1.371 (8)
C (25) -H (25)	0.9300
C (26) -C (27)	1.358 (7)
C (26) -H (26)	0.9300
C (27) -C (28)	1.358 (6)
C (27) -H (27)	0.9300
C (28) -C (29)	1.364 (6)

C(28)-H(28)	0.9300
C(29)-C(30)	1.483(6)
C(30)-N(31)	1.279(5)
C(30)-N(40)	1.341(6)
N(31)-N(32)	1.423(4)
N(32)-S(33)	1.638(4)
N(32)-H(32)	0.93(5)
S(33)-O(41)	1.416(3)
S(33)-O(42)	1.430(3)
S(33)-C(34)	1.756(4)
C(34)-C(35)	1.366(5)
C(34)-C(39)	1.376(6)
C(35)-C(36)	1.371(6)
C(35)-H(35)	0.9300
C(36)-C(37)	1.383(6)
C(36)-H(36)	0.9300
C(37)-C(38)	1.392(6)
C(37)-C(43)	1.509(7)

C(38) - C(39)	1.373 (7)
C(38) - H(38)	0.9300
C(39) - H(39)	0.9300
N(40) - H(40A)	0.77 (4)
N(40) - H(40B)	1.02 (8)
C(43) - C(45)	1.453 (11)
C(43) - C(44)	1.497 (8)
C(43) - C(46)	1.593 (14)
C(44) - H(44A)	0.9600
C(44) - H(44B)	0.9600
C(44) - H(44C)	0.9600
C(45) - H(45A)	0.9600
C(45) - H(45B)	0.9600
C(45) - H(45C)	0.9600
C(46) - H(46A)	0.9600
C(46) - H(46B)	0.9600
C(46) - H(46C)	0.9600
C(2) - N(1) - C(6)	116.2 (4)

N(1) - C(2) - C(3)	124.8 (5)
N(1) - C(2) - H(2)	117.6
C(3) - C(2) - H(2)	117.6
C(2) - C(3) - C(4)	118.9 (4)
C(2) - C(3) - H(3)	120.6
C(4) - C(3) - H(3)	120.6
C(3) - C(4) - C(5)	117.8 (4)
C(3) - C(4) - H(4)	121.1
C(5) - C(4) - H(4)	121.1
C(4) - C(5) - C(6)	119.4 (4)
C(4) - C(5) - H(5)	120.3
C(6) - C(5) - H(5)	120.3
N(1) - C(6) - C(5)	122.9 (3)
N(1) - C(6) - C(7)	114.6 (3)
C(5) - C(6) - C(7)	122.5 (3)
N(8) - C(7) - N(17)	126.4 (3)
N(8) - C(7) - C(6)	116.3 (3)
N(17) - C(7) - C(6)	117.2 (3)

C(7) -N(8) -N(9)	110.7 (3)
N(8) -N(9) -S(10)	113.7 (2)
N(8) -N(9) -H(9)	115 (3)
S(10) -N(9) -H(9)	109 (3)
O(18) -S(10) -O(19)	119.03 (18)
O(18) -S(10) -N(9)	107.61 (17)
O(19) -S(10) -N(9)	103.74 (16)
O(18) -S(10) -C(11)	108.38 (17)
O(19) -S(10) -C(11)	108.55 (17)
N(9) -S(10) -C(11)	109.17 (16)
C(12) -C(11) -C(16)	120.2 (4)
C(12) -C(11) -S(10)	119.5 (3)
C(16) -C(11) -S(10)	120.3 (3)
C(11) -C(12) -C(13)	119.3 (4)
C(11) -C(12) -H(12)	120.4
C(13) -C(12) -H(12)	120.4
C(14) -C(13) -C(12)	121.9 (4)
C(14) -C(13) -H(13)	119.1

C(12) - C(13) - H(13)	119.1
C(13) - C(14) - C(15)	117.1 (4)
C(13) - C(14) - C(20)	123.3 (4)
C(15) - C(14) - C(20)	119.6 (4)
C(16) - C(15) - C(14)	122.2 (4)
C(16) - C(15) - H(15)	118.9
C(14) - C(15) - H(15)	118.9
C(15) - C(16) - C(11)	119.4 (4)
C(15) - C(16) - H(16)	120.3
C(11) - C(16) - H(16)	120.3
C(7) - N(17) - H(17A)	119 (2)
C(7) - N(17) - H(17B)	119 (4)
H(17A) - N(17) - H(17B)	122 (5)
C(23) - C(20) - C(22)	113.6 (5)
C(23) - C(20) - C(14)	109.8 (5)
C(22) - C(20) - C(14)	111.6 (4)
C(23) - C(20) - C(21)	106.1 (5)
C(22) - C(20) - C(21)	106.7 (5)

C(14) - C(20) - C(21)	108.8 (4)
C(20) - C(21) - H(21A)	109.5
C(20) - C(21) - H(21B)	109.5
H(21A) - C(21) - H(21B)	109.5
C(20) - C(21) - H(21C)	109.5
H(21A) - C(21) - H(21C)	109.5
H(21B) - C(21) - H(21C)	109.5
C(20) - C(22) - H(22A)	109.5
C(20) - C(22) - H(22B)	109.5
H(22A) - C(22) - H(22B)	109.5
C(20) - C(22) - H(22C)	109.5
H(22A) - C(22) - H(22C)	109.5
H(22B) - C(22) - H(22C)	109.5
C(20) - C(23) - H(23A)	109.5
C(20) - C(23) - H(23B)	109.5
H(23A) - C(23) - H(23B)	109.5
C(20) - C(23) - H(23C)	109.5
H(23A) - C(23) - H(23C)	109.5

H(23B) - C(23) - H(23C)	109.5
C(25) - N(24) - C(29)	117.6 (5)
N(24) - C(25) - C(26)	124.0 (5)
N(24) - C(25) - H(25)	118.0
C(26) - C(25) - H(25)	118.0
C(27) - C(26) - C(25)	117.9 (5)
C(27) - C(26) - H(26)	121.1
C(25) - C(26) - H(26)	121.1
C(28) - C(27) - C(26)	119.0 (5)
C(28) - C(27) - H(27)	120.5
C(26) - C(27) - H(27)	120.5
C(27) - C(28) - C(29)	120.2 (4)
C(27) - C(28) - H(28)	119.9
C(29) - C(28) - H(28)	119.9
N(24) - C(29) - C(28)	121.3 (4)
N(24) - C(29) - C(30)	116.1 (4)
C(28) - C(29) - C(30)	122.6 (4)
N(31) - C(30) - N(40)	126.5 (4)

N(31) -C(30) -C(29)	117.8(3)
N(40) -C(30) -C(29)	115.7(4)
C(30) -N(31) -N(32)	111.7(3)
N(31) -N(32) -S(33)	113.9(3)
N(31) -N(32) -H(32)	112(3)
S(33) -N(32) -H(32)	106(3)
O(41) -S(33) -O(42)	119.39(19)
O(41) -S(33) -N(32)	108.29(19)
O(42) -S(33) -N(32)	103.6(2)
O(41) -S(33) -C(34)	108.57(19)
O(42) -S(33) -C(34)	107.59(18)
N(32) -S(33) -C(34)	108.98(17)
C(35) -C(34) -C(39)	120.0(4)
C(35) -C(34) -S(33)	119.8(3)
C(39) -C(34) -S(33)	120.1(3)
C(34) -C(35) -C(36)	119.2(4)
C(34) -C(35) -H(35)	120.4
C(36) -C(35) -H(35)	120.4

C(35) - C(36) - C(37)	123.0 (4)
C(35) - C(36) - H(36)	118.5
C(37) - C(36) - H(36)	118.5
C(36) - C(37) - C(38)	116.2 (4)
C(36) - C(37) - C(43)	120.3 (4)
C(38) - C(37) - C(43)	123.6 (4)
C(39) - C(38) - C(37)	121.7 (4)
C(39) - C(38) - H(38)	119.2
C(37) - C(38) - H(38)	119.2
C(38) - C(39) - C(34)	120.0 (4)
C(38) - C(39) - H(39)	120.0
C(34) - C(39) - H(39)	120.0
C(30) - N(40) - H(40A)	122 (3)
C(30) - N(40) - H(40B)	104 (4)
H(40A) - N(40) - H(40B)	132 (5)
C(45) - C(43) - C(44)	113.1 (7)
C(45) - C(43) - C(37)	110.4 (7)
C(44) - C(43) - C(37)	113.5 (5)

C(45) - C(43) - C(46)	108.3 (9)
C(44) - C(43) - C(46)	103.1 (7)
C(37) - C(43) - C(46)	107.9 (6)
C(43) - C(44) - H(44A)	109.5
C(43) - C(44) - H(44B)	109.5
H(44A) - C(44) - H(44B)	109.5
C(43) - C(44) - H(44C)	109.5
H(44A) - C(44) - H(44C)	109.5
H(44B) - C(44) - H(44C)	109.5
C(43) - C(45) - H(45A)	109.5
C(43) - C(45) - H(45B)	109.5
H(45A) - C(45) - H(45B)	109.5
C(43) - C(45) - H(45C)	109.5
H(45A) - C(45) - H(45C)	109.5
H(45B) - C(45) - H(45C)	109.5
C(43) - C(46) - H(46A)	109.5
C(43) - C(46) - H(46B)	109.5
H(46A) - C(46) - H(46B)	109.5

C(43) - C(46) - H(46C)	109.5
H(46A) - C(46) - H(46C)	109.5
H(46B) - C(46) - H(46C)	109.5

Table 4. Anisotropic displacement parameters ($\text{\AA}^2 \times 10^3$) for dr944rfr. The anisotropic displacement factor exponent takes the form: $-2 \pi^2 [h^2 a^2 U_{11} + \dots + 2 h k a^* b^* U_{12}]$.

	U11	U22	U33	U23	U13	U12
N(1)	40 (2)	134 (4)	59 (2)	-35 (2)	17 (2)	-20 (2)
C(2)	41 (2)	239 (8)	79 (3)	-72 (4)	26 (2)	-31 (3)
C(3)	44 (2)	195 (7)	78 (3)	-48 (4)	29 (2)	-4 (3)
C(4)	63 (3)	113 (4)	57 (3)	-26 (3)	24 (2)	2 (3)
C(5)	46 (2)	67 (2)	55 (2)	-12 (2)	15 (2)	-7 (2)
C(6)	35 (2)	59 (2)	42 (2)	-1 (2)	11 (1)	-2 (2)
C(7)	36 (2)	40 (2)	41 (2)	1 (1)	10 (1)	-2 (1)
N(8)	36 (1)	54 (2)	45 (2)	-5 (1)	16 (1)	0 (1)
N(9)	32 (1)	57 (2)	44 (2)	-8 (2)	12 (1)	-1 (1)
S(10)	32 (1)	45 (1)	54 (1)	-9 (1)	6 (1)	5 (1)
C(11)	34 (2)	50 (2)	49 (2)	-7 (2)	9 (1)	-1 (1)
C(12)	61 (2)	54 (2)	49 (2)	-12 (2)	22 (2)	-13 (2)
C(13)	79 (3)	57 (2)	61 (3)	-20 (2)	34 (2)	-18 (2)
C(14)	65 (2)	55 (2)	71 (3)	-15 (2)	24 (2)	-12 (2)

C(15)	92 (3)	59 (3)	72 (3)	-6 (2)	39 (3)	-18 (2)
C(16)	76 (3)	60 (2)	60 (2)	-15 (2)	34 (2)	-7 (2)
N(17)	32 (2)	65 (2)	54 (2)	-16 (2)	13 (1)	-5 (1)
O(18)	59 (2)	53 (2)	70 (2)	2 (1)	-1 (1)	12 (1)
O(19)	41 (1)	70 (2)	83 (2)	-30 (2)	23 (1)	3 (1)
C(20)	101 (4)	55 (3)	103 (4)	-19 (3)	39 (3)	-27 (3)
C(21)	169 (7)	63 (3)	111 (5)	3 (3)	41 (5)	1 (4)
C(22)	213 (8)	60 (3)	122 (5)	-37 (3)	86 (5)	-26 (4)
C(23)	136 (6)	94 (4)	146 (6)	-11 (4)	41 (5)	-57 (4)
N(24)	125 (4)	79 (3)	54 (2)	-6 (2)	10 (2)	-25 (3)
C(25)	162 (6)	95 (4)	46 (3)	-21 (3)	9 (3)	-22 (4)
C(26)	103 (4)	97 (4)	59 (3)	6 (3)	31 (3)	15 (3)
C(27)	69 (3)	85 (3)	65 (3)	5 (3)	25 (2)	1 (2)
C(28)	61 (2)	69 (3)	53 (2)	-3 (2)	17 (2)	-1 (2)
C(29)	61 (2)	52 (2)	49 (2)	-3 (2)	6 (2)	4 (2)
C(30)	58 (2)	53 (2)	50 (2)	2 (2)	10 (2)	-3 (2)
N(31)	55 (2)	57 (2)	44 (2)	1 (2)	13 (1)	4 (2)
N(32)	57 (2)	61 (2)	46 (2)	4 (2)	12 (1)	9 (2)

S(33)	57(1)	66(1)	41(1)	2(1)	14(1)	16(1)
C(34)	57(2)	50(2)	42(2)	0(2)	11(2)	8(2)
C(35)	58(2)	47(2)	67(3)	12(2)	15(2)	2(2)
C(36)	58(2)	55(2)	80(3)	19(2)	12(2)	8(2)
C(37)	65(3)	61(3)	78(3)	16(2)	5(2)	-4(2)
C(38)	83(3)	52(2)	94(4)	13(2)	16(3)	-6(2)
C(39)	73(3)	52(2)	76(3)	13(2)	15(2)	16(2)
N(40)	137(5)	106(4)	58(3)	3(3)	14(3)	-62(3)
O(41)	75(2)	74(2)	68(2)	-6(2)	15(2)	30(2)
O(42)	68(2)	107(2)	45(2)	9(2)	20(1)	14(2)
C(43)	63(3)	100(4)	173(7)	51(4)	11(4)	-19(3)
C(44)	93(4)	114(5)	125(5)	41(4)	25(4)	-26(4)
C(45)	103(6)	412(19)	266(13)	251(14)	-83(7)	-122(9)
C(46)	102(6)	136(8)	560(30)	-17(12)	161(11)	2(5)

Table 5. Hydrogen coordinates ($\times 10^4$) and isotropic displacement parameters ($\text{\AA}^2 \times 10^3$) for dr944rfr.

	x	y	z	U(eq)
H(2)	-1347	5568	1074	142
H(3)	-1043	6429	1974	124
H(4)	911	7042	2395	91
H(5)	2485	6715	1871	67
H(9)	4150 (40)	5930 (20)	240 (20)	54 (12)
H(12)	5710	6873	2140	64
H(13)	5957	8263	2364	75
H(15)	6793	8601	585	85
H(16)	6487	7232	336	75
H(17A)	2570 (40)	5110 (20)	-10 (20)	56 (11)

H(17B)	1250 (50)	5240 (30)	60 (30)	98 (18)
H(21A)	4855	9842	942	170
H(21B)	5960	9824	589	170
H(21C)	5826	10564	1062	170
H(22A)	5247	9614	2185	186
H(22B)	6149	10374	2286	186
H(22C)	6617	9538	2650	186
H(23A)	7956	10344	1743	187
H(23B)	8060	9625	1244	187
H(23C)	8418	9474	2036	187
H(25)	8703	4790	5132	125
H(26)	7671	3748	5514	102
H(27)	6625	2783	4736	86
H(28)	6665	2898	3611	73
H(32)	6780 (50)	4240 (30)	1720 (30)	88 (16)
H(35)	4462	4066	1009	69
H(36)	2379	3851	907	78
H(38)	3051	1503	1429	93

H(39)	5146	1720	1555	82
H(40A)	8490 (40)	4780 (30)	2530 (20)	55 (13)
H(40B)	8670 (70)	4980 (50)	3340 (40)	150 (30)
H(44A)	1363	1616	1768	167
H(44B)	726	1324	1019	167
H(44C)	-61	1792	1443	167
H(45A)	852	3061	161	427
H(45B)	-406	2965	374	427
H(45C)	218	2195	133	427
H(46A)	1136	3132	2025	378
H(46B)	-217	3142	1533	378
H(46C)	800	3755	1412	378
